Space and time-resolved X-ray spectroscopy technique by CCD pinhole camera

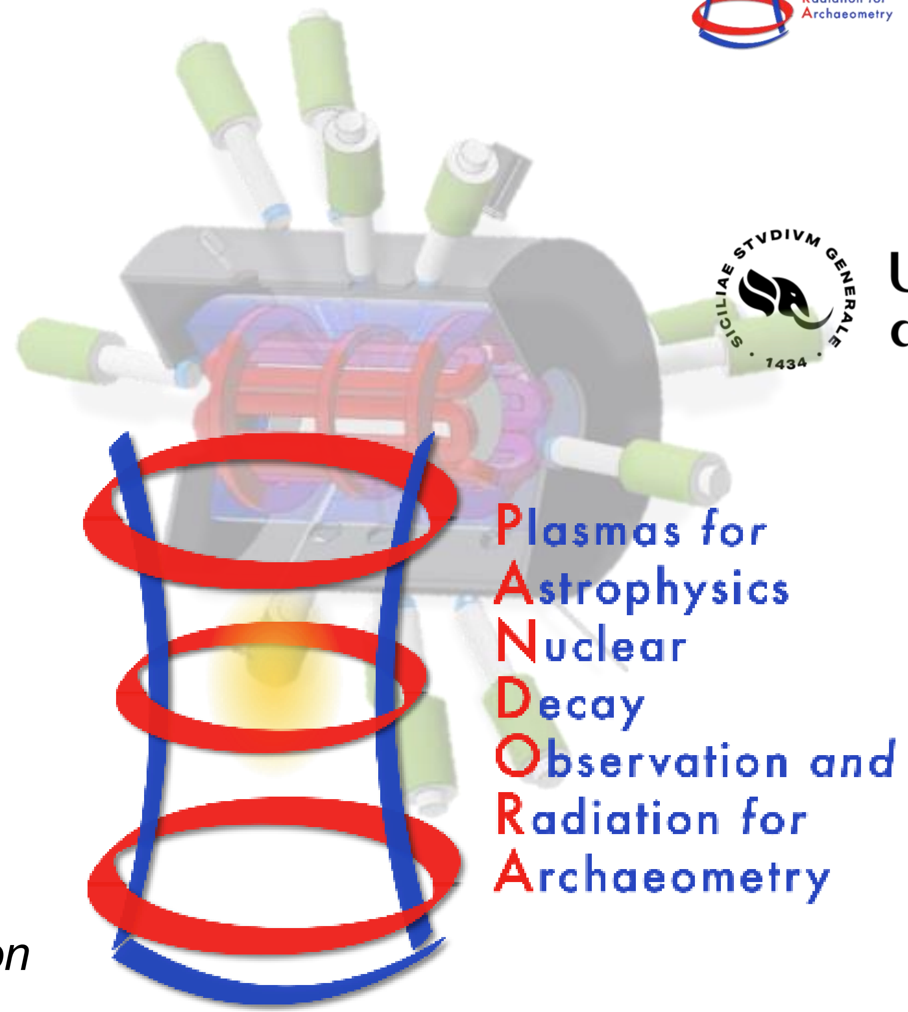

Giorgio Finocchiaro *on behalf of the PANDORA collaboration*

Istituto Nazionale di Fisica Nucleare – Laboratori Nazionali del Sud – Catania (Italy)

Plasmas for Astrophysics Nuclear Decay Observation and Radiation for Archaeometry

INFN LNS
Istituto Nazionale di Fisica Nucleare
Laboratori Nazionali del Sud

Outline

- Introduction: X-ray imaging on ECR plasmas
- Single-photon-counting technique on CCD detectors
- Energy calibration by XRF test-bench
- ECR plasma imaging at Atomki laboratory:
  Space and time resolved application

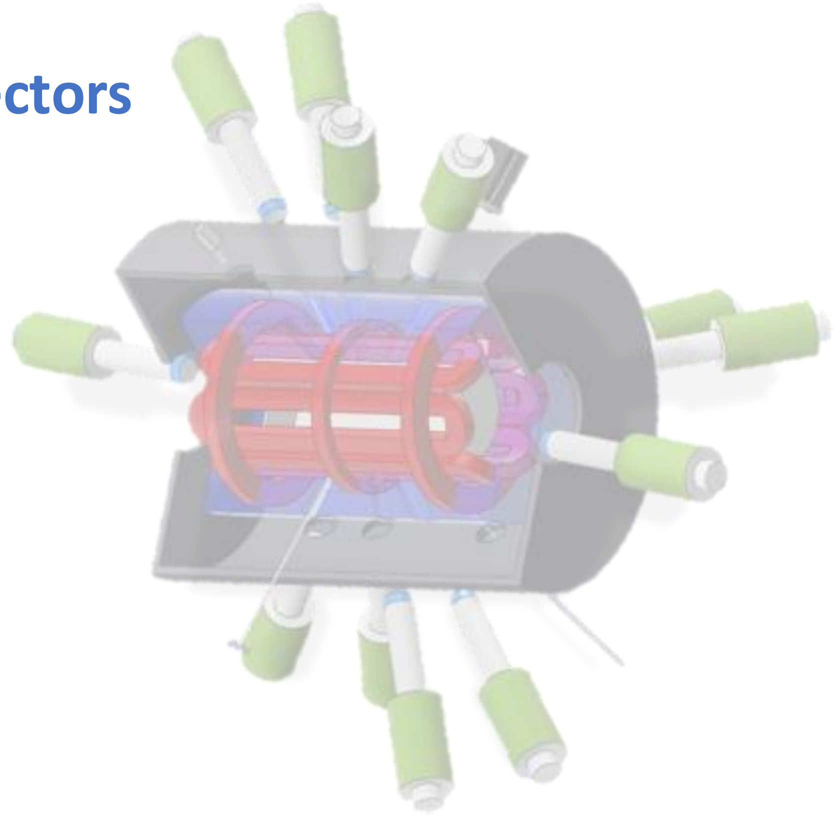

Introduction

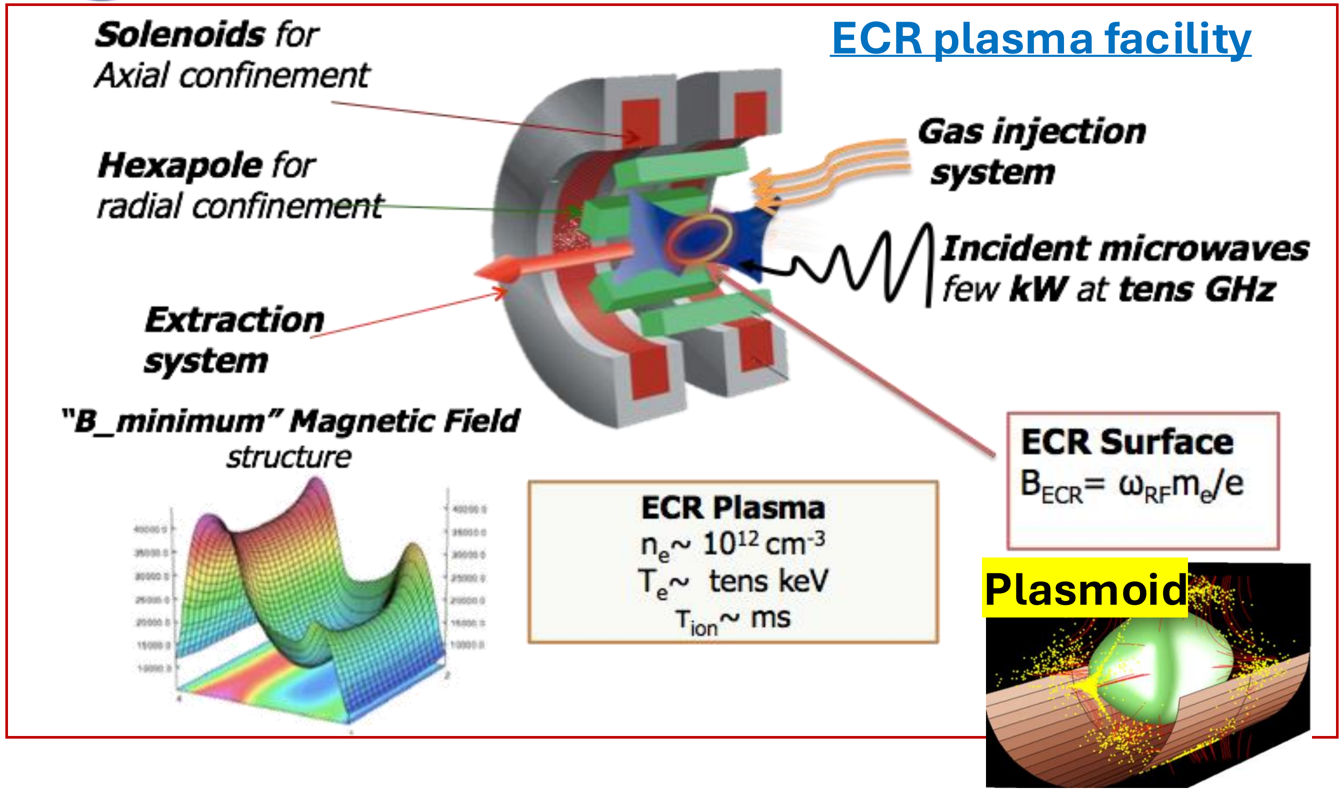

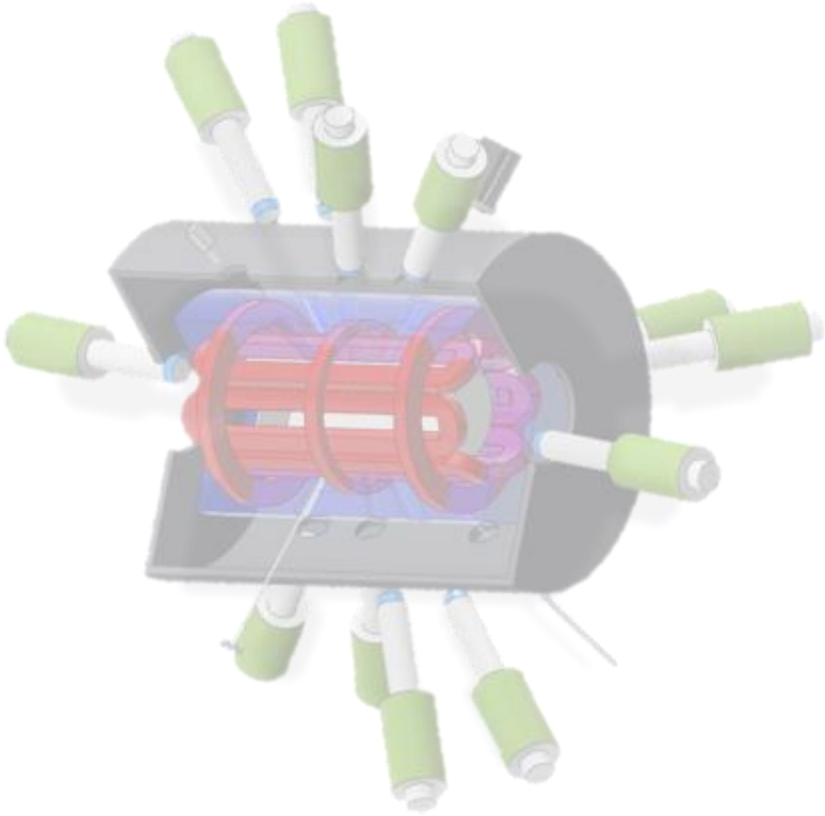

The X-ray diagnostics is an insightful technique to monitor the self-emission of magnetically confined plasmas.

High **emissivity** in the soft X-ray **energy range (0.5 - 30 keV)**: **$J \sim 10^{11}$ cm^{-3}s^{-1}**

Introduction

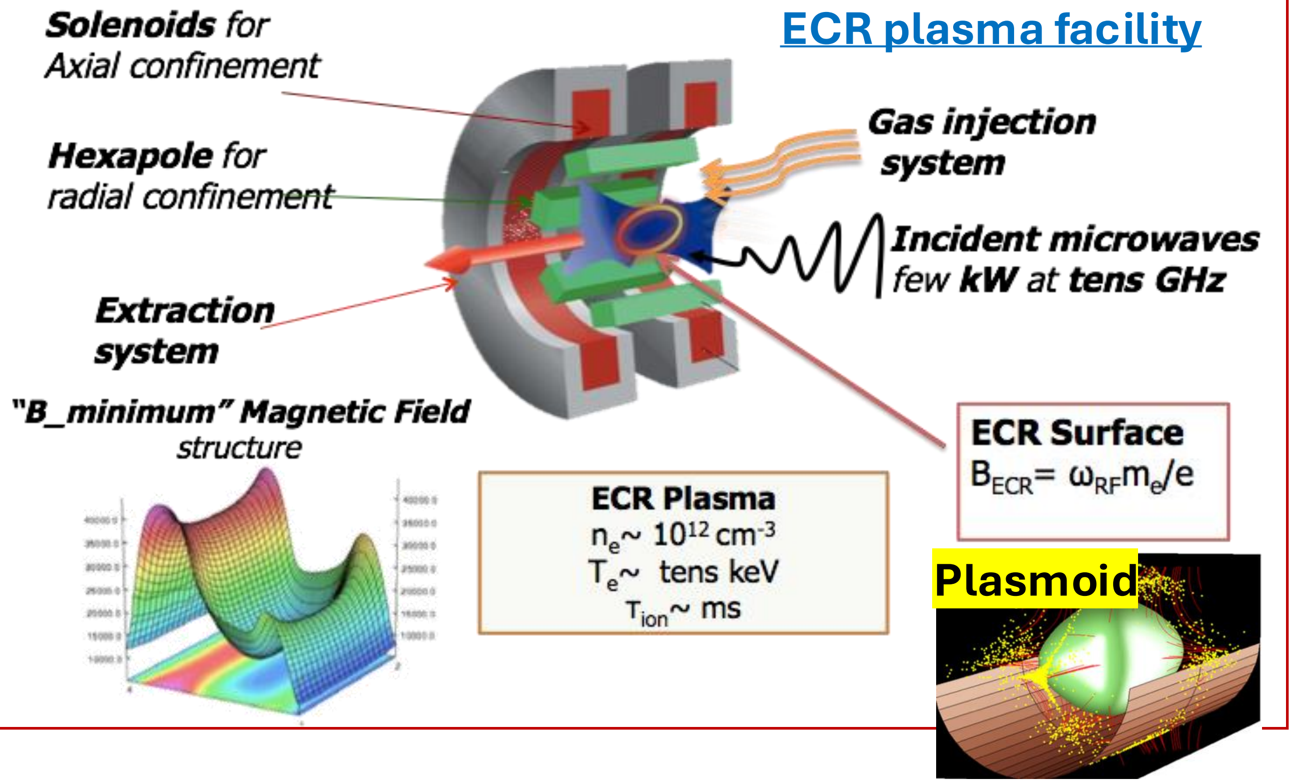

The X-ray diagnostics is an insightful technique to monitor the self-emission of magnetically confined plasmas.

High **emissivity** in the soft X-ray **energy range (0.5 - 30 keV)**: **$J \sim 10^{11}$ cm^{-3}s^{-1}**

Laboratory plasma can become an **environment** for Nuclear Astrophysics research (β decay investigation)

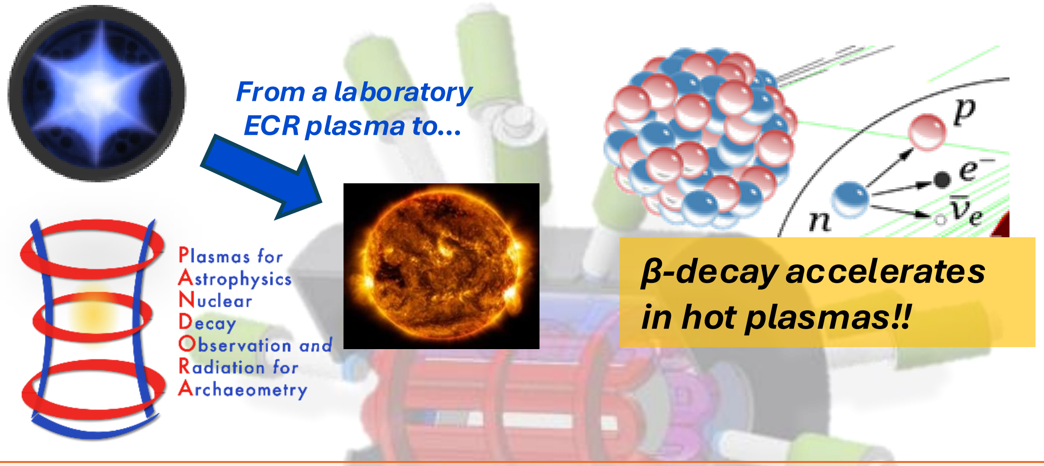

X-ray imaging of ECR (electron cyclotron resonance) plasma:

- ✓ Plasma confinement investigation and optimization
- ✓ Non-invasive measurement of thermodynamic parameters
- ✓ Monitoring of plasma stability during long measurements

Energy-resolved imaging by X-ray CCD detectors

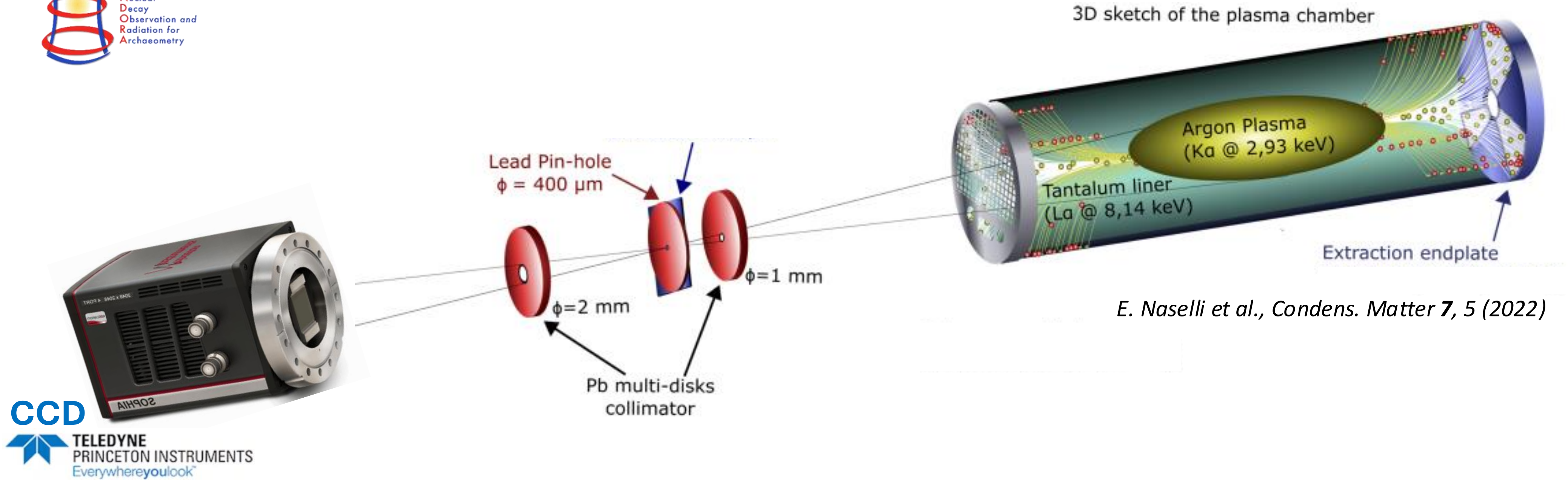

E. Naselli et al., Condens. Matter ***7****, 5 (2022)*

- Back-illuminated CCD sensors with >95% QE (~5 eV to 30 keV range)
- 2k x 2k formats; 13.5 micron pixels
- High frame rates with up to 4-port readout
- Cooling down to -90°C using liquid or air

Energy-resolved imaging by X-ray CCD detectors

Plasmas for Astrophysics Nuclear Decay Observation and Radiation for Archaeometry

INFN LNS
Istituto Nazionale di Fisica Nucleare
Laboratori Nazionali del Sud

atomki DEBRECEN

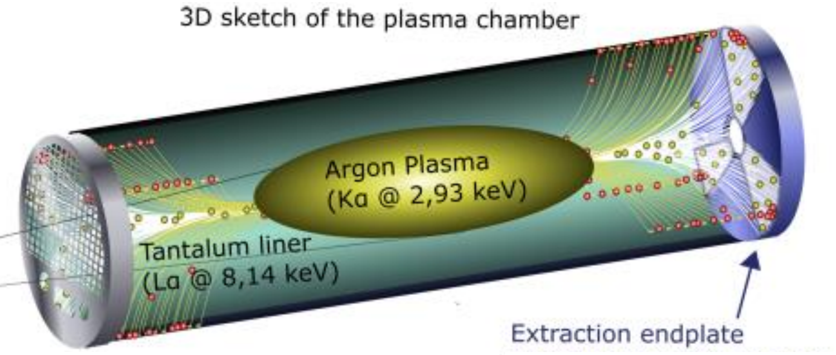

E. Naselli et al., Condens. Matter ***7****, 5 (2022)*

Pin-hole camera + shutter

Pb multi-disks collimator

CCD

TELEDYNE PRINCETON INSTRUMENTS
Everywhereyoulook™

- Back-illuminated CCD sensors with >95% QE (~5 eV to 30 keV range)
- 2k x 2k formats; 13.5 micron pixels
- High frame rates with up to 4-port readout
- Cooling down to -90°C using liquid or air

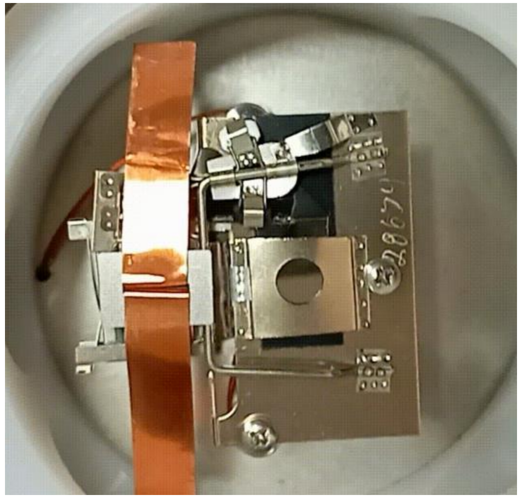

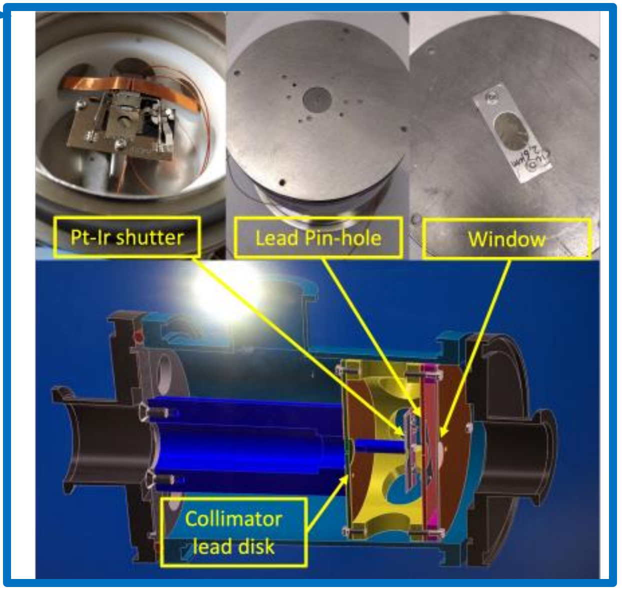

Plasmas for Astrophysics Nuclear Decay Observation and Radiation for Archaeometry

Energy-resolved imaging by X-ray CCD detectors

INFN LNS
Istituto Nazionale di Fisica Nucleare
Laboratori Nazionali del Sud

atomki DEBRECEN

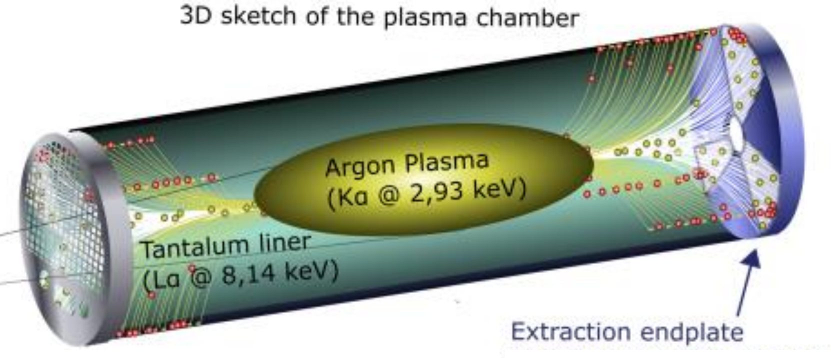

E. Naselli et al., Condens. Matter ***7***, *5 (2022)*

Pin-hole camera + shutter

CCD

TELEDYNE PRINCETON INSTRUMENTS
Everywhereyoulook™

- Back-illuminated CCD sensors with >95% QE (~5 eV to 30 keV range)
- 2k x 2k formats; 13.5 micron pixels
- High frame rates with up to 4-port readout
- Cooling down to -90°C using liquid or air

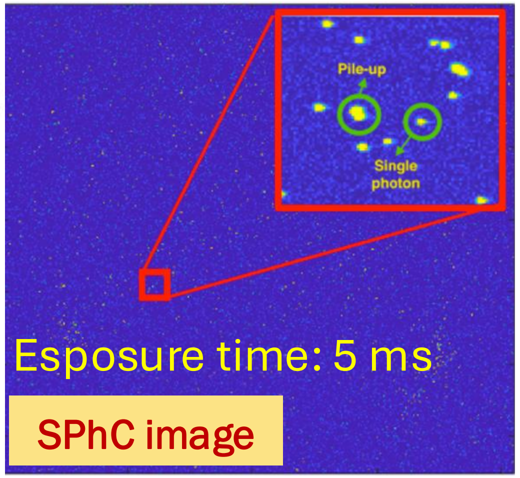

A graphic algorithm identifies **single-photon events** on CCD images to perform **space-resolved spectroscopy**

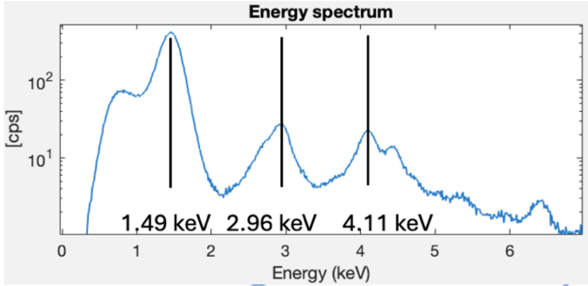

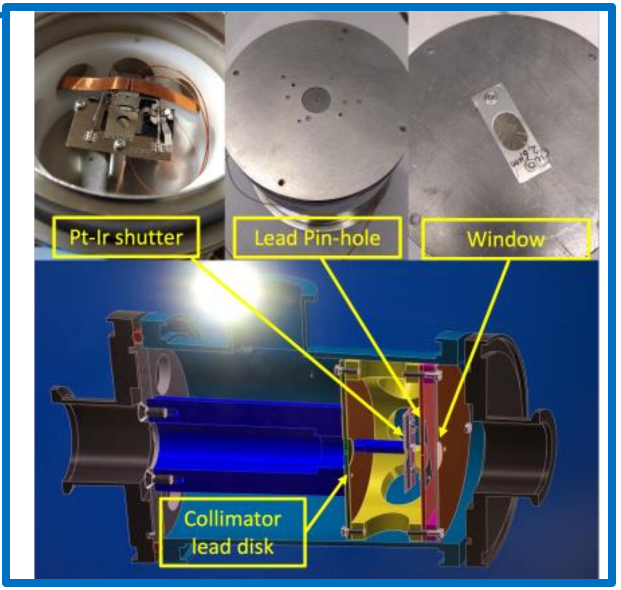

Plasmas for Astrophysics Nuclear Decay Observation and Radiation for Archaeometry

INFN LNS
Istituto Nazionale di Fisica Nucleare
Laboratori Nazionali del Sud

SPhC reconstruction technique

CCD
TELEDYNE PRINCETON INSTRUMENTS
Everywhereyoulook

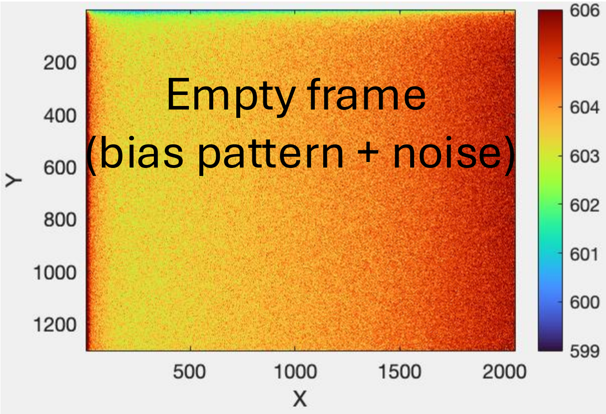

Readout noise distribution

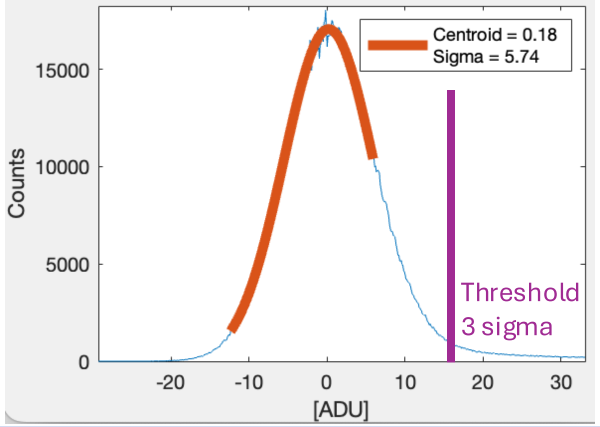

SPhC clusters identification

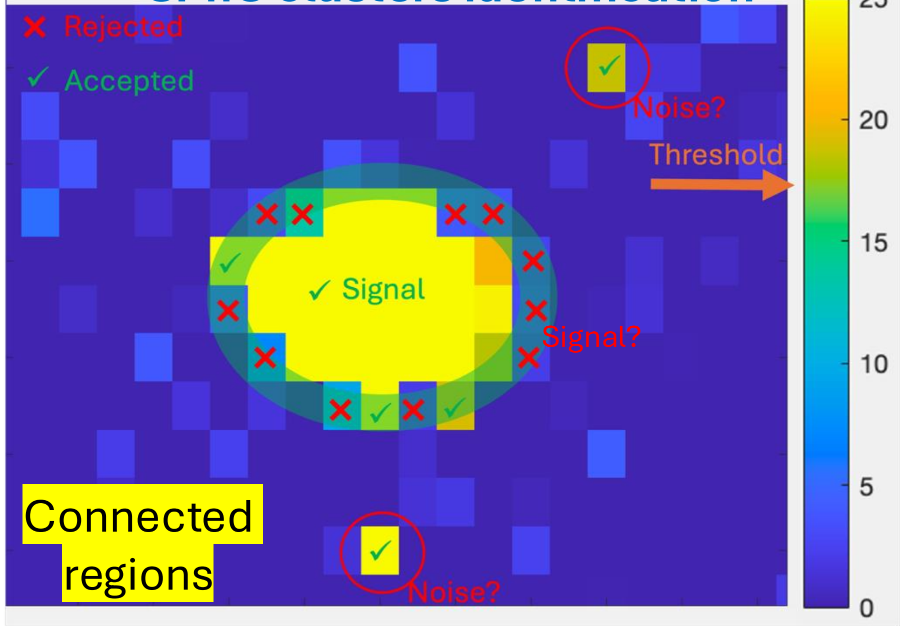

Geometrical features of single-photon clusters

- Sum (digitized collected charge summed over area)
- X, Y centroid position
- Eccentricity, Major and minor axis of a fitting ellipse
- Number of local maxima

The SPhC algorithm **identifies** the connected regions above threshold, extracting relevant geometrical features.

The **noise-threshold** value trades-off unwanted multi-event connection with a partial loss of energy information.

Pile-up events are recognized and discarded.

Energy integration

Detector characterization by XRF test bench

CCD

TELEDYNE PRINCETON INSTRUMENTS Everywhereyoulook

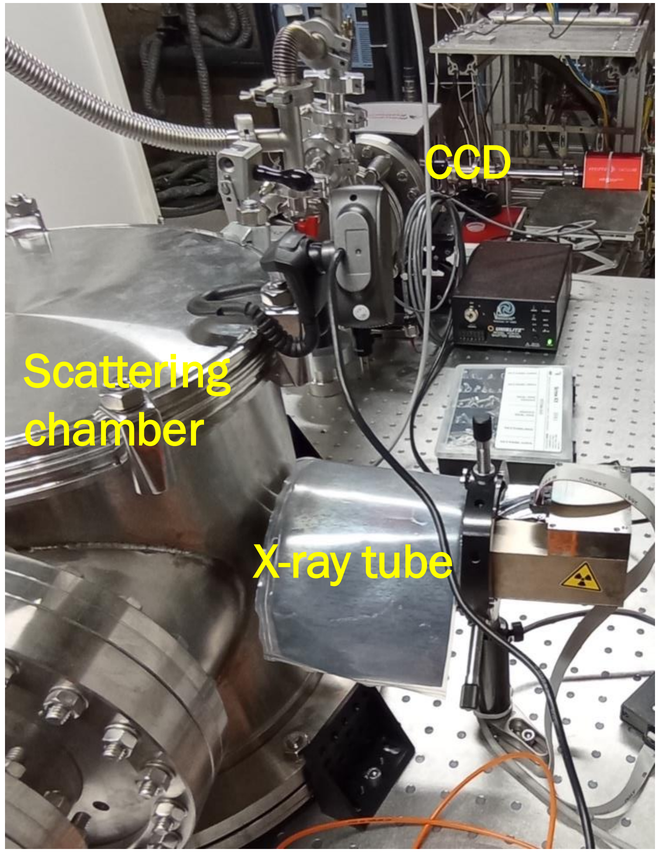

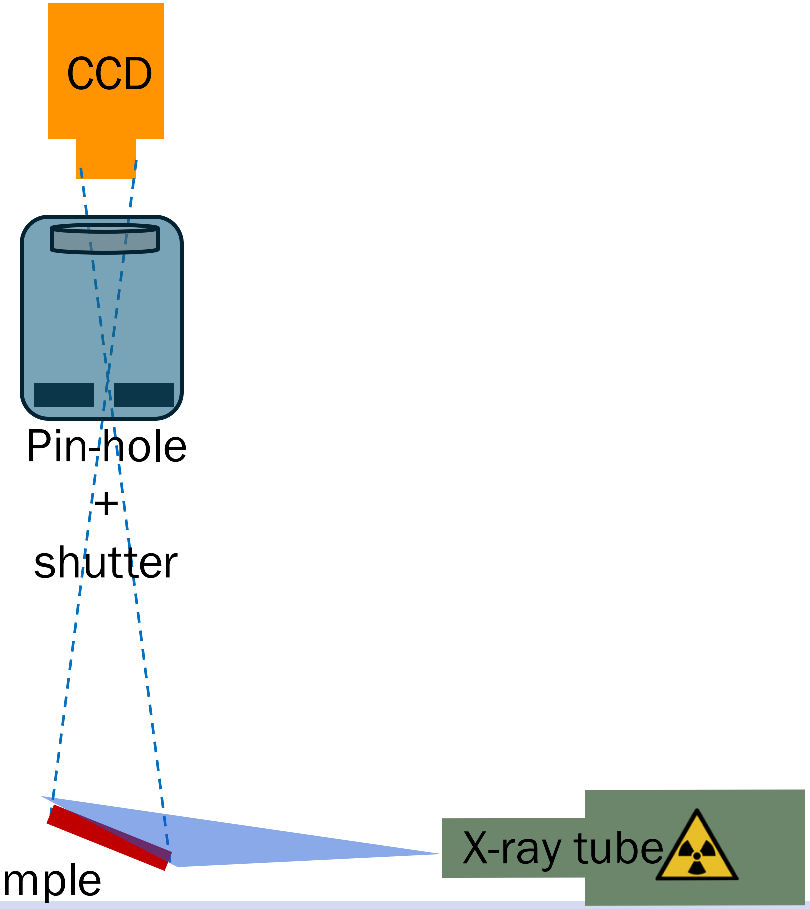

Detector characterization by XRF test bench

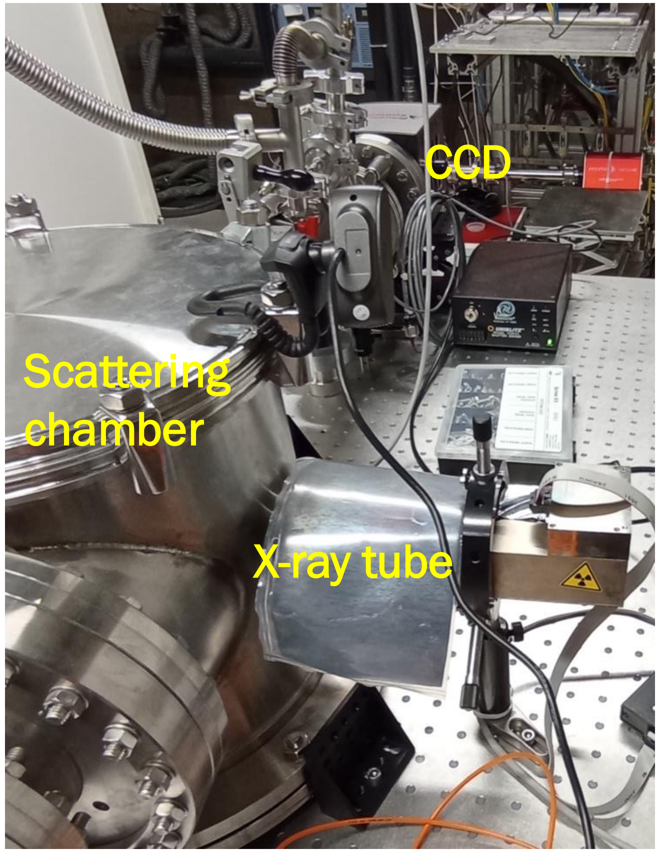

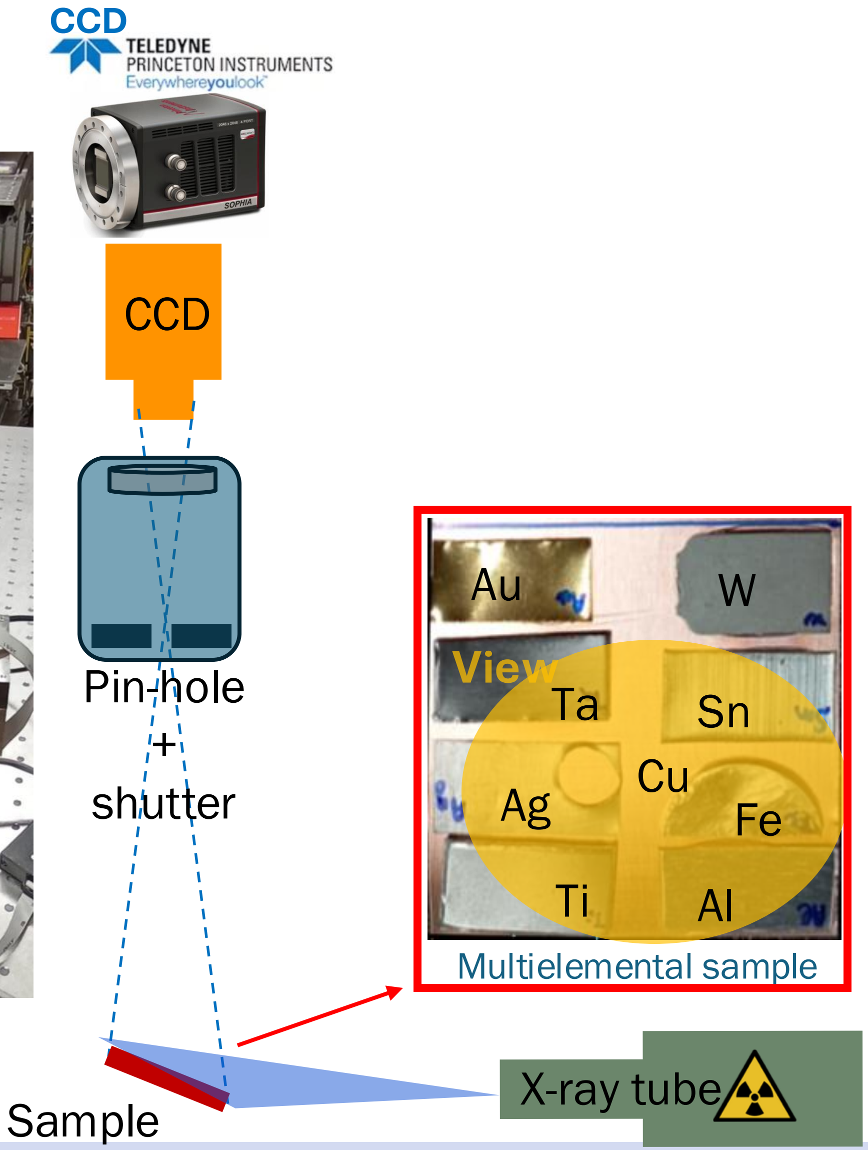

Multielemental sample

Detector characterization by XRF test bench

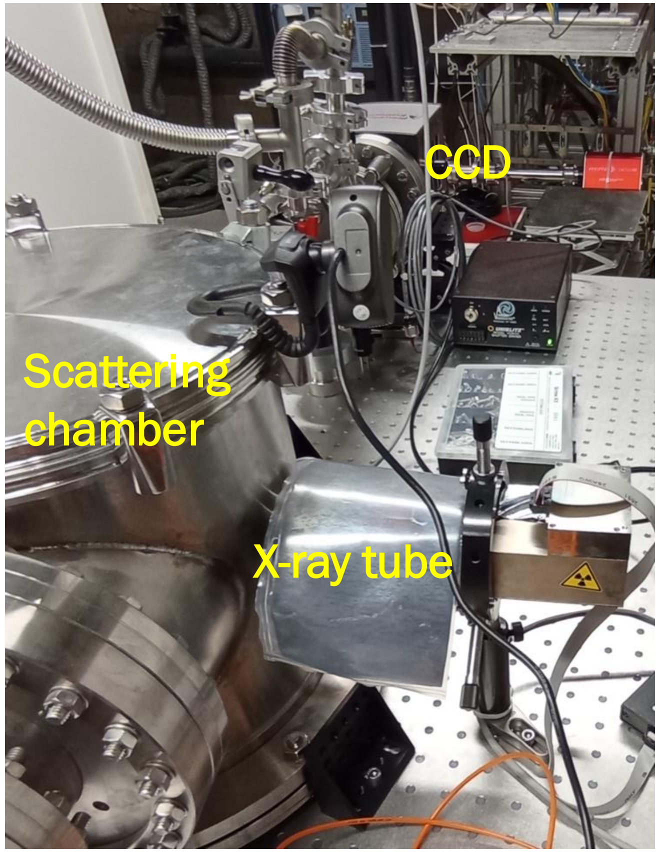

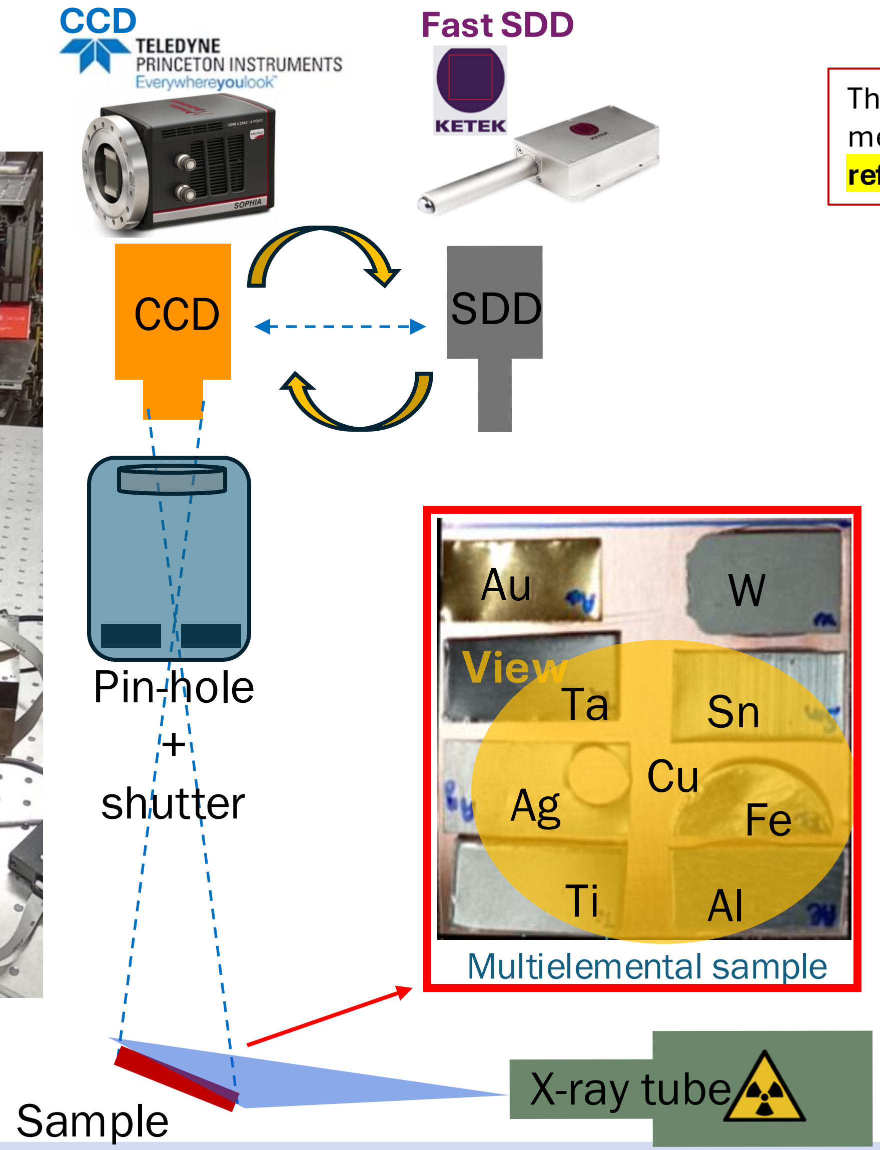

The sample emission induced by the X-ray source has been measured with both the CCD and the **SDD detector** as a **reference**, in the same optical conditions

Detector characterization by XRF test bench

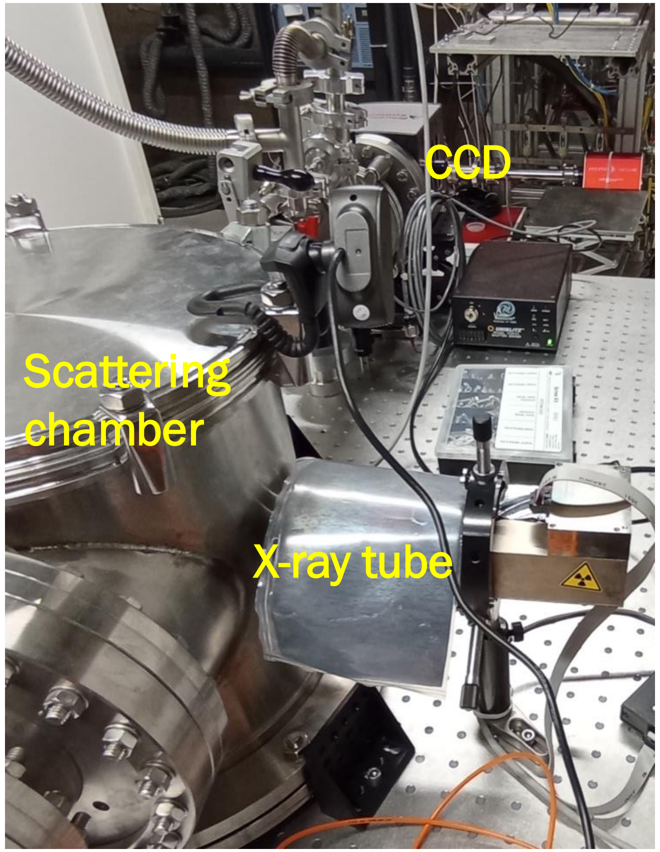

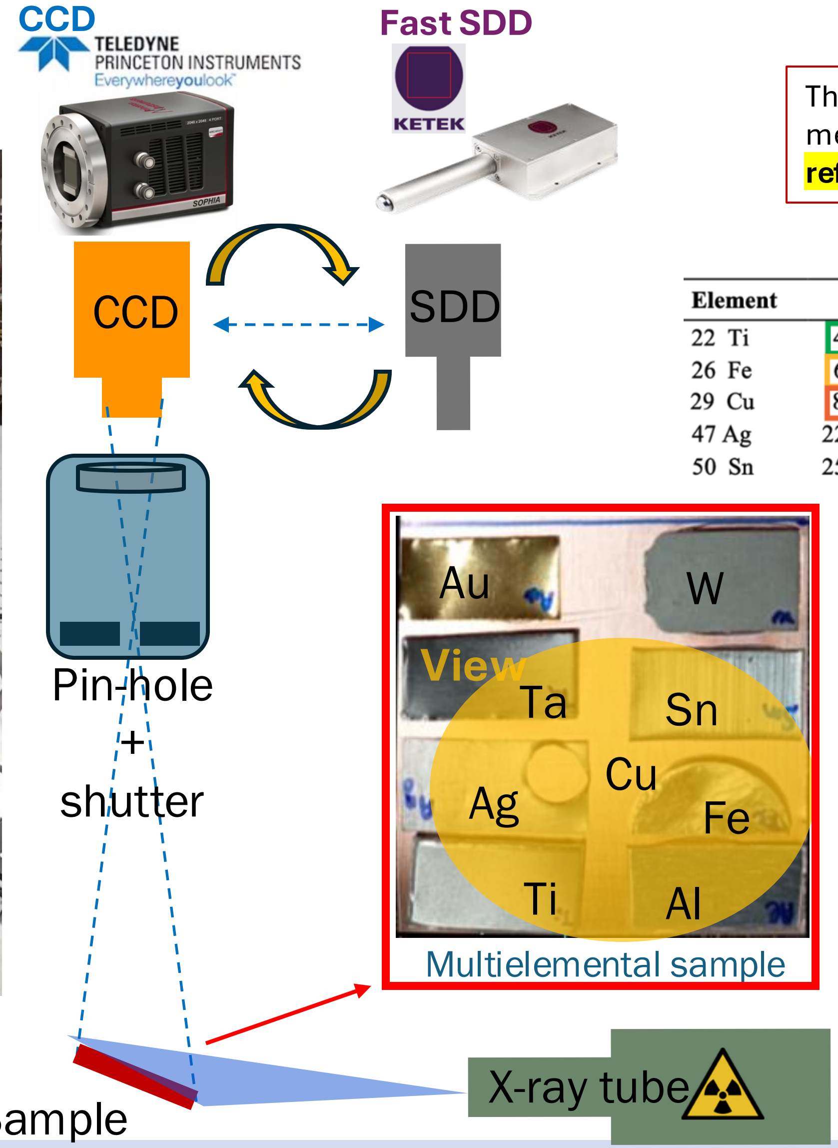

The sample emission induced by the X-ray source has been measured with both the CCD and the **SDD detector** as a **reference**, in the same optical conditions

Fluorescence emission table

Element	$K\alpha_1$	$K\alpha_2$	$K\beta_1$	$L\alpha_1$	$L\alpha_2$	$L\beta_1$	$L\beta_2$	$L\gamma_1$
22 Ti	4,510.84	4,504.86	4,931.81	452.2	452.2	458.4		
26 Fe	6,403.84	6,390.84	7,057.98	705.0	705.0	718.5		
29 Cu	8,047.78	8,027.83	8,905.29	929.7	929.7	949.8		
47 Ag	22,162.92	21,990.3	24,942.4	2,984.31	2,978.21	3,150.94	3,347.81	3,519.59
50 Sn	25,271.3	25,044.0	28,486.0	3,443.98	3,435.42	3,662.80	3,904.86	4,131.12

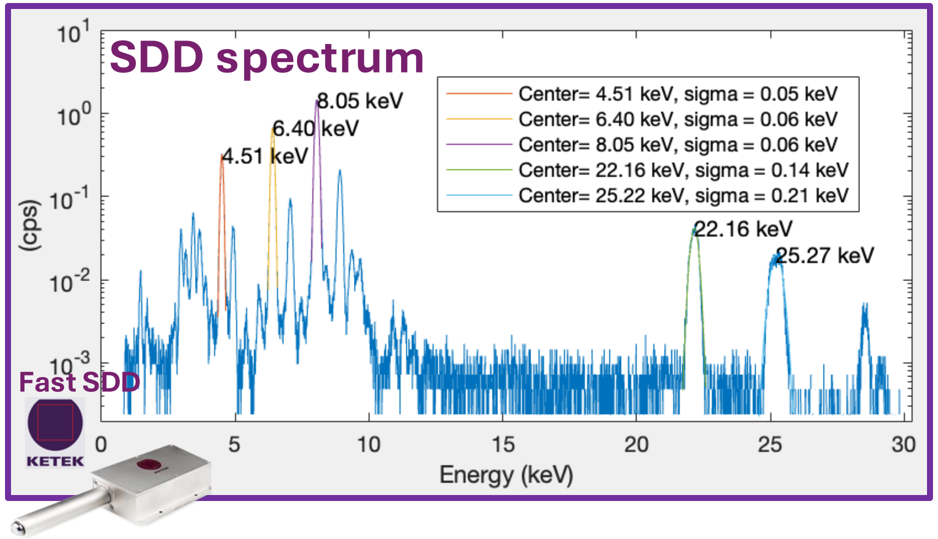

Detector characterization by XRF test bench

CCD

TELEDYNE PRINCETON INSTRUMENTS
Everywhereyoulook

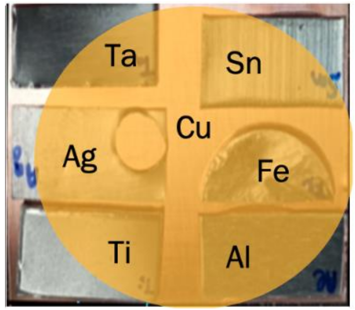

Element	$K\alpha_1$	$K\alpha_2$	$K\beta_1$	$L\alpha_1$	$L\alpha_2$	$L\beta_1$	$L\beta_2$	$L\gamma_1$
22 Ti	4,510.84	4,504.86	4,931.81	452.2	452.2	458.4		
26 Fe	6,403.84	6,390.84	7,057.98	705.0	705.0	718.5		
29 Cu	8,047.78	8,027.83	8,905.29	929.7	929.7	949.8		
47 Ag	22,162.92	21,990.3	24,942.4	2,984.31	2,978.21	3,150.94	3,347.81	3,519.59
50 Sn	25,271.3	25,044.0	28,486.0	3,443.98	3,435.42	3,662.80	3,904.86	4,131.12

The CCD energy calibration is challenging!

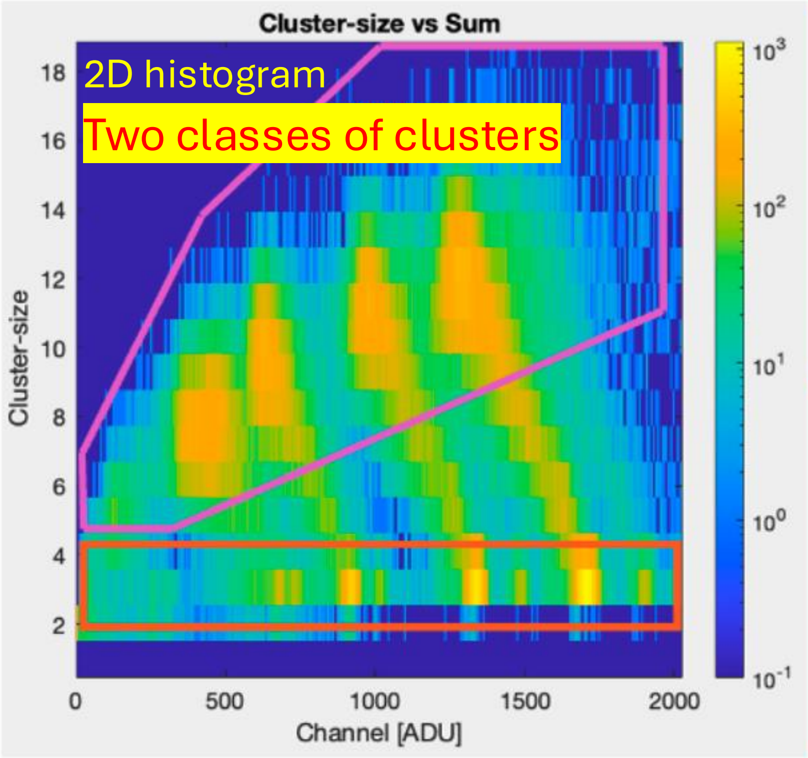

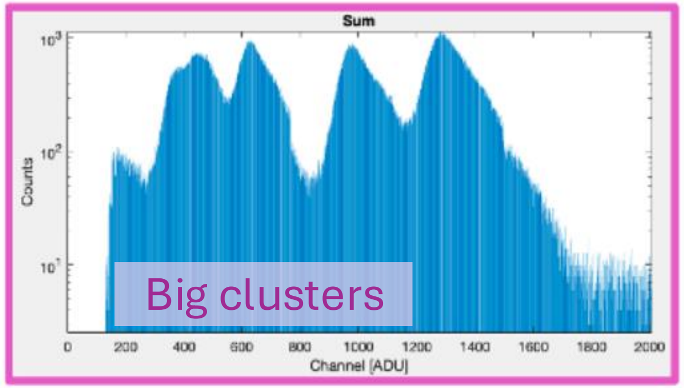

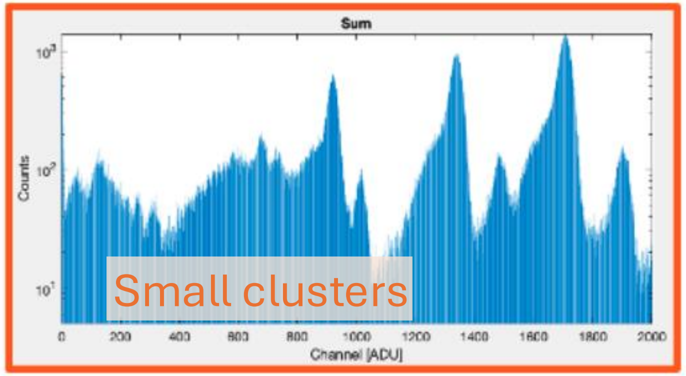

A charge collection **artifact** is observed in the reconstruction of the energy information.
The fluorescence is still resolved on a parametric 2D histogram.

Plasmas for Astrophysics Nuclear Decay Observation and Radiation for Archaeometry

Detector characterization by XRF test bench

Istituto Nazionale di Fisica Nucleare
Laboratori Nazionali del Sud

CCD
TELEDYNE PRINCETON INSTRUMENTS
Everywhereyoulook

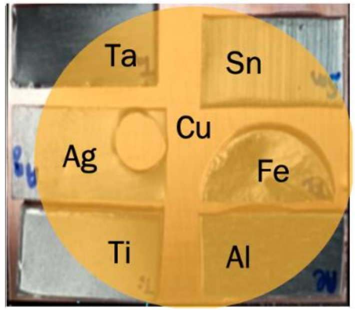

Element	$K\alpha_1$	$K\alpha_2$	$K\beta_1$	$L\alpha_1$	$L\alpha_2$	$L\beta_1$	$L\beta_2$	$L\gamma_1$
22 Ti	4,510.84	4,504.86	4,931.81	452.2	452.2	458.4		
26 Fe	6,403.84	6,390.84	7,057.98	705.0	705.0	718.5		
29 Cu	8,047.78	8,027.83	8,905.29	929.7	929.7	949.8		
47 Ag	22,162.92	21,990.3	24,942.4	2,984.31	2,978.21	3,150.94	3,347.81	3,519.59
50 Sn	25,271.3	25,044.0	28,486.0	3,443.98	3,435.42	3,662.80	3,904.86	4,131.12

The CCD energy calibration is challenging!

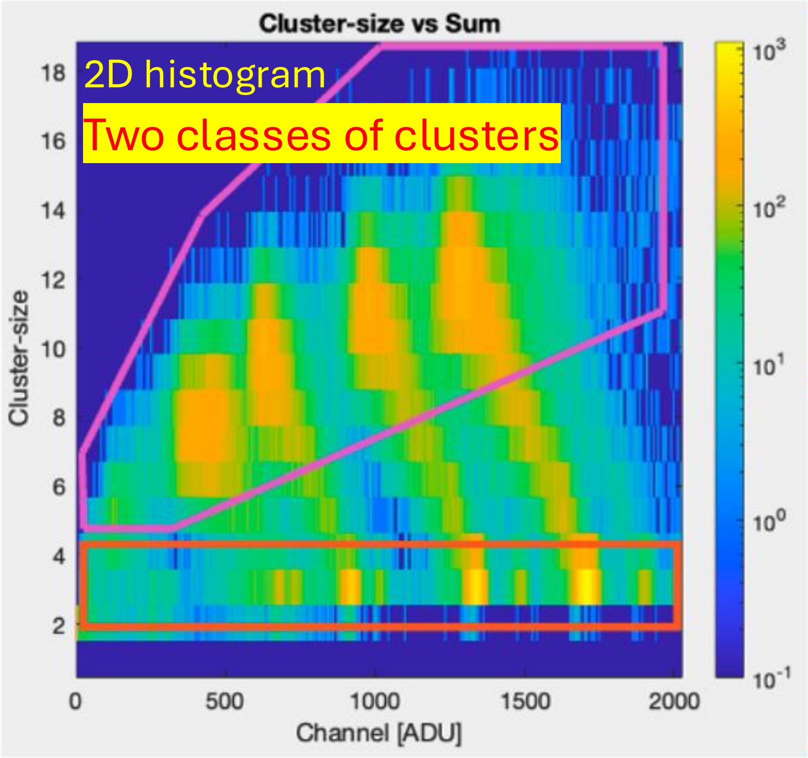

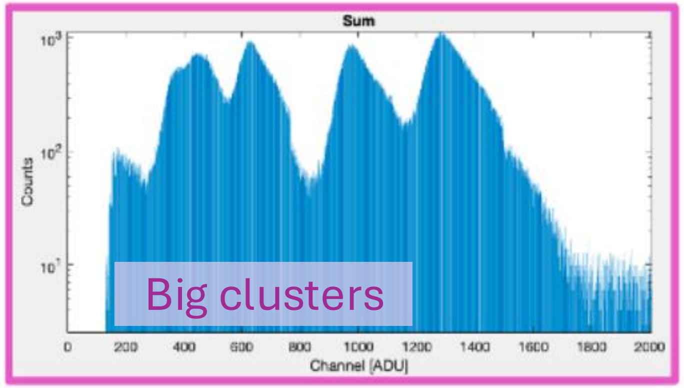

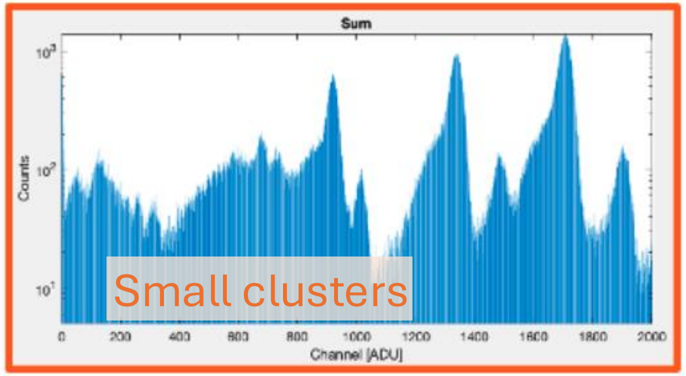

A charge collection **artifact** is observed in the reconstruction of the energy information.
The fluorescence is still resolved on a parametric 2D histogram.

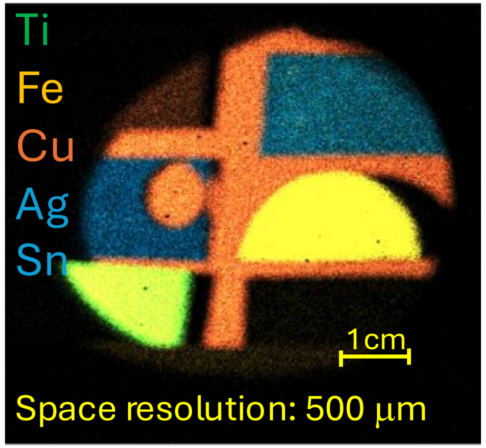

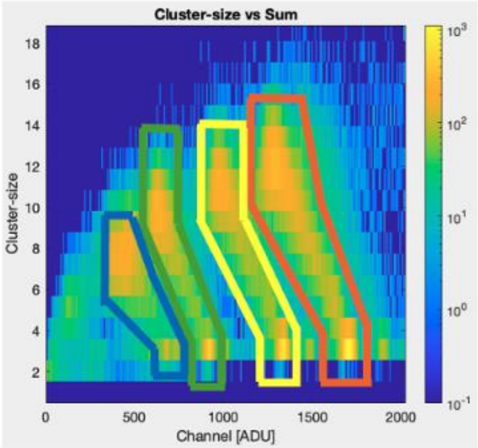

✓ Imaging check

Plasmas for Astrophysics Nuclear Decay Observation and Radiation for Archaeometry

Detector characterization by XRF test bench

Istituto Nazionale di Fisica Nucleare
Laboratori Nazionali del Sud

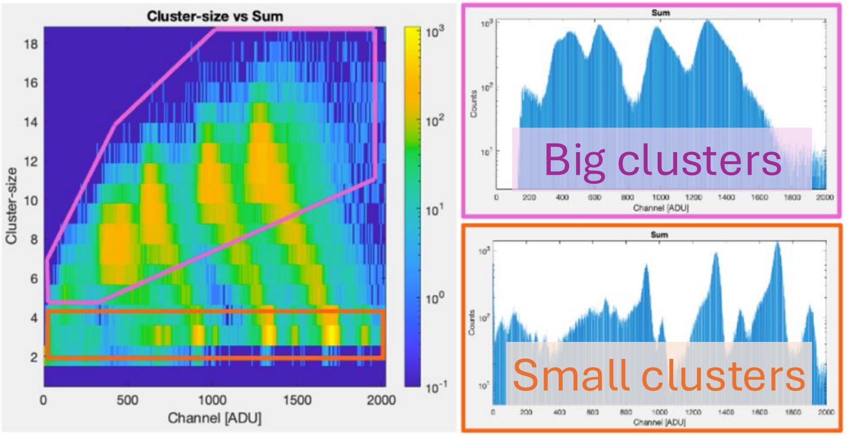

The same effect is reproduced in Monte Carlo simulations

MC simulation

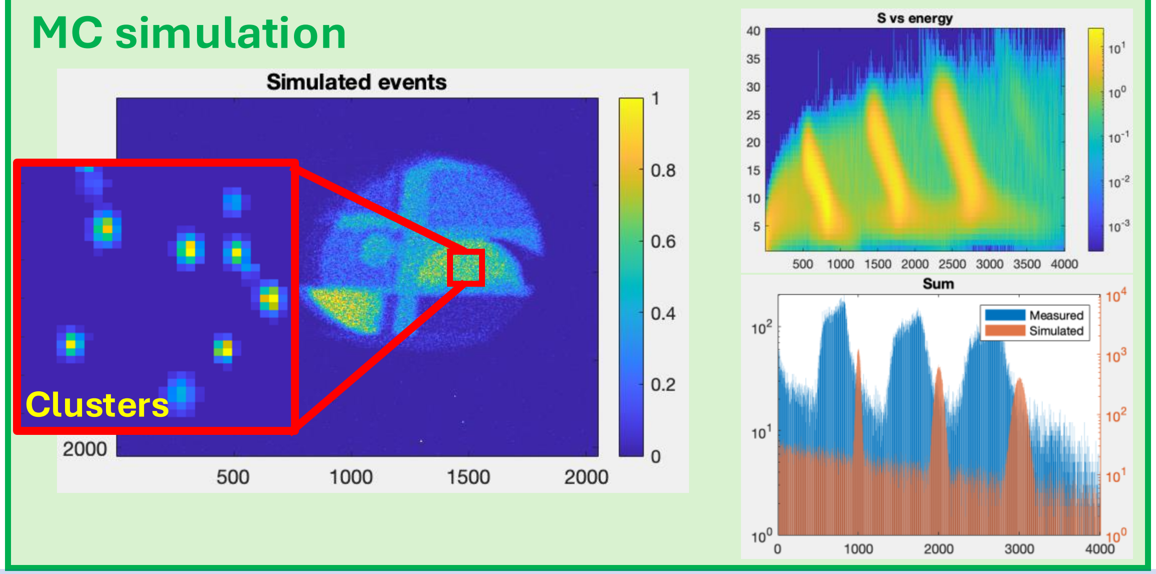

Detector characterization by XRF test bench

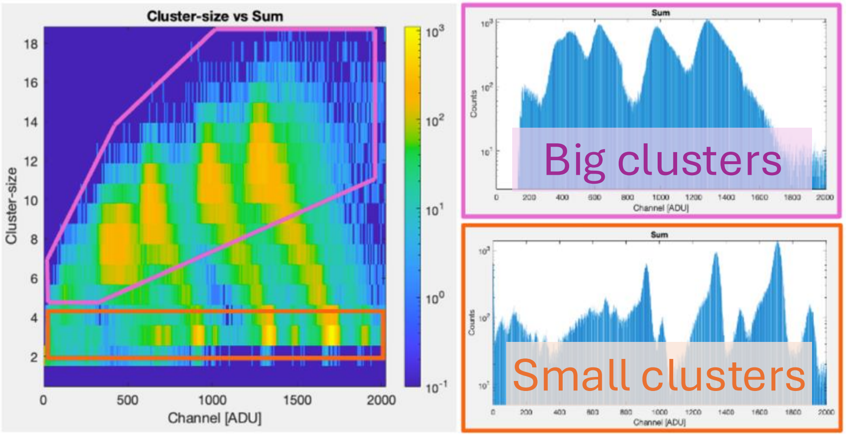

The same effect is reproduced in Monte Carlo simulations

MC simulation

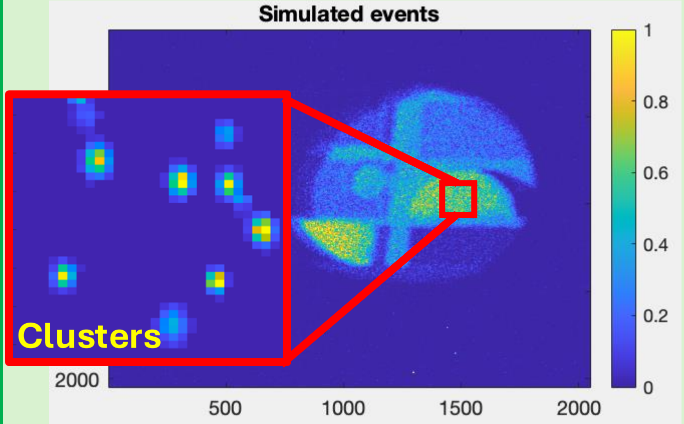

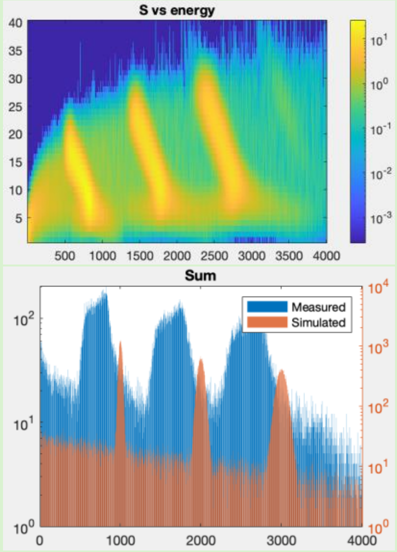

Extension of the integration domain (under noise threshold)

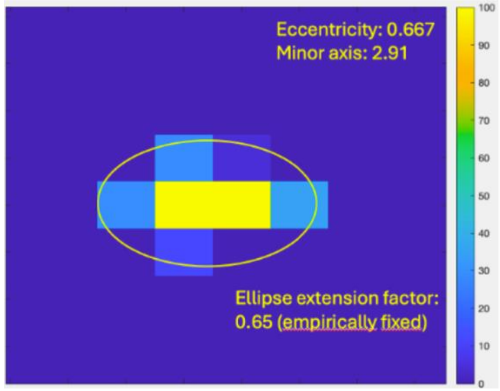

Trade-off with energy resolution!

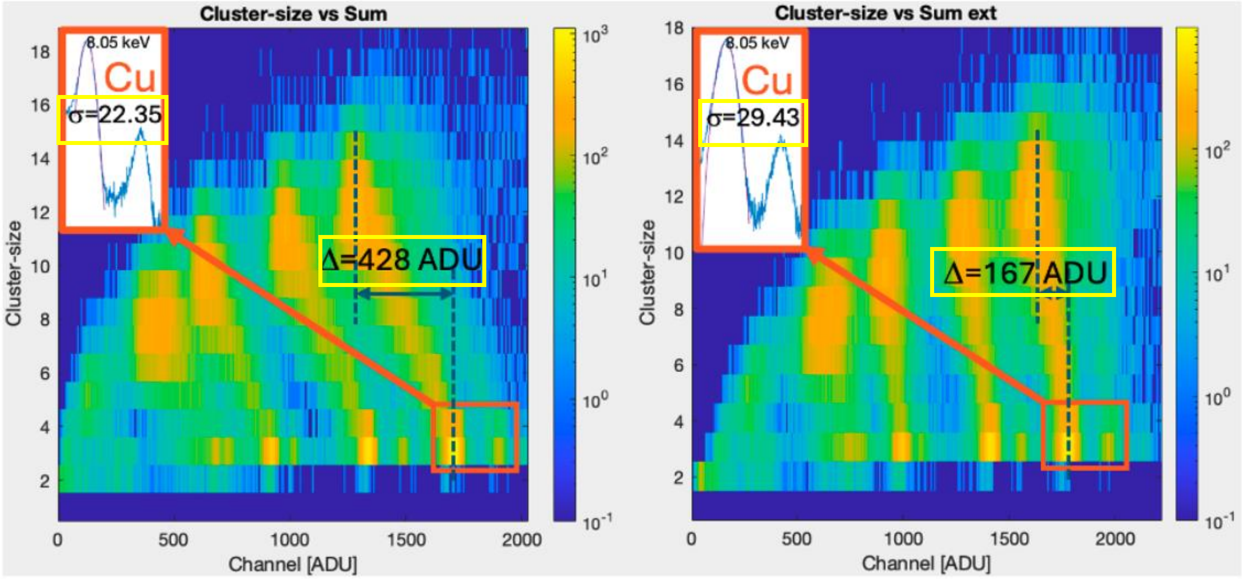

Detector characterization by XRF test bench

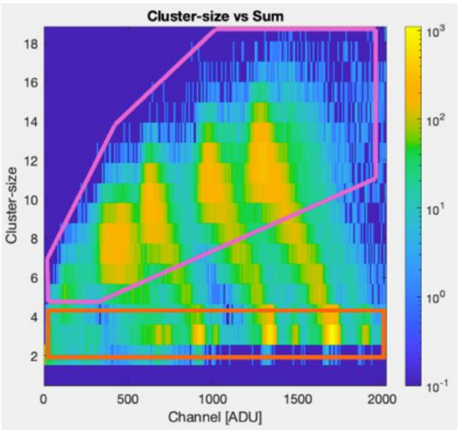

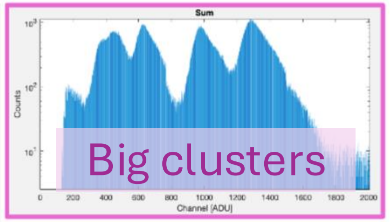

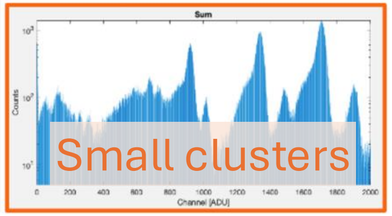

The same effect is reproduced in Monte Carlo simulations

Suggested talk about AI-based algorithm: Bianca Peri

Extension of the integration domain (under noise threshold)

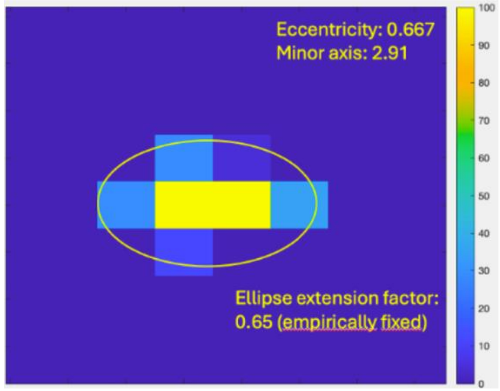

MC simulation

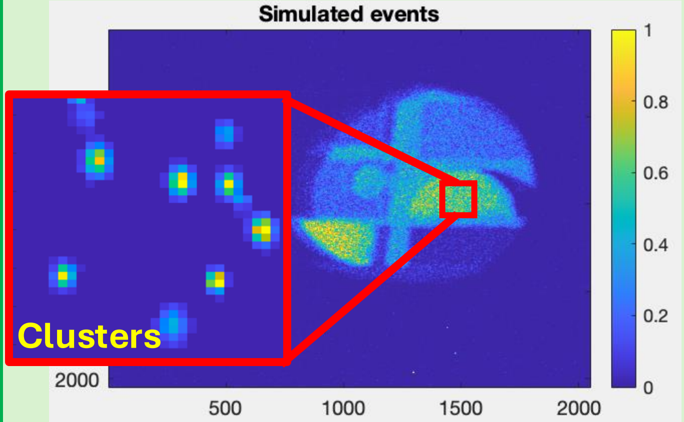

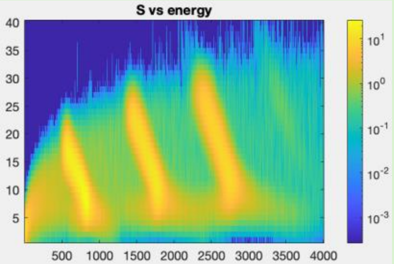

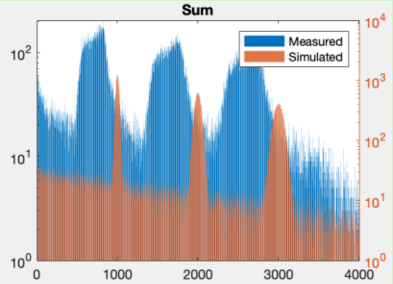

Trade-off with energy resolution!

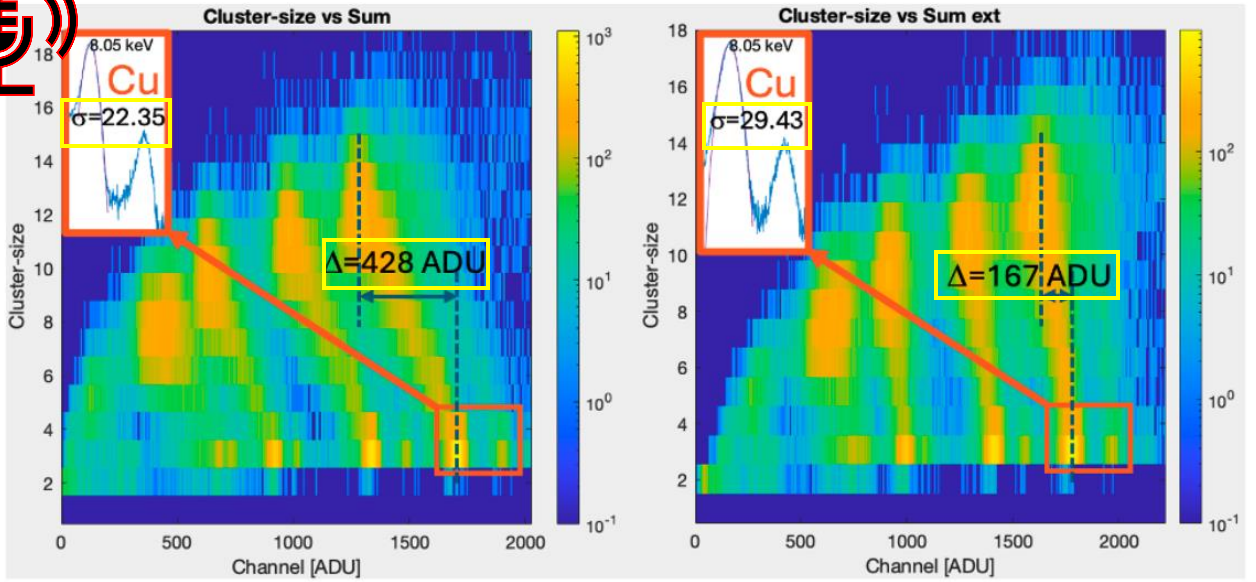

Plasmas for Astrophysics Nuclear Decay Observation and Radiation for Archaeometry

Multi-parameteric energy calibration

Istituto Nazionale di Fisica Nucleare
Laboratori Nazionali del Sud

The energy calibration of the two classes is performed in different ways.

Small clusters → linear energy calibration

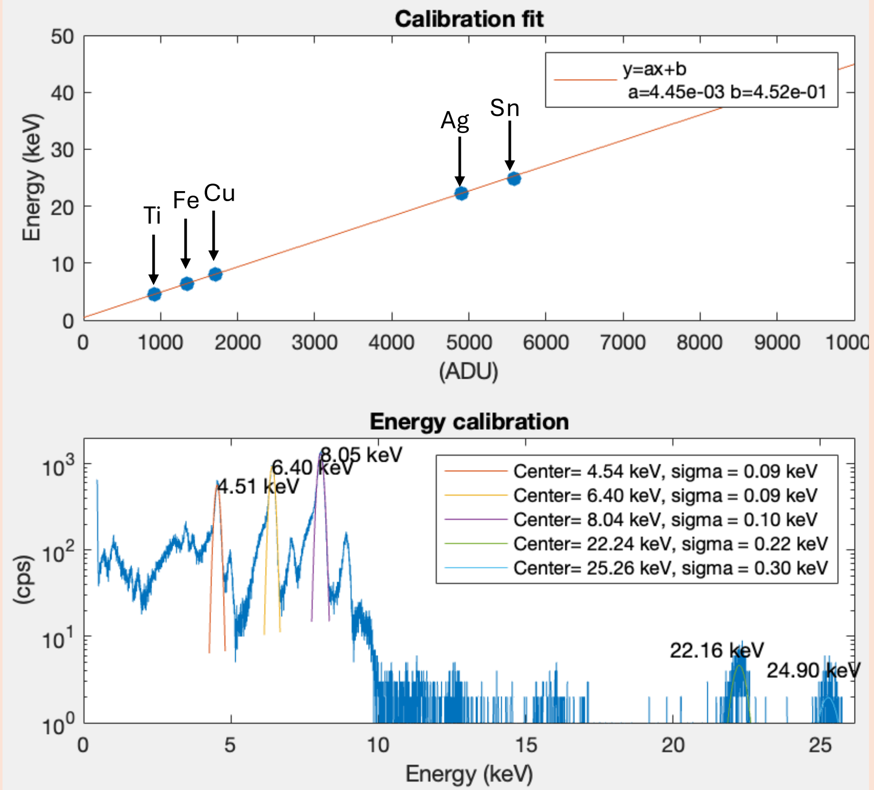

FWHM=236 eV @ 8 keV

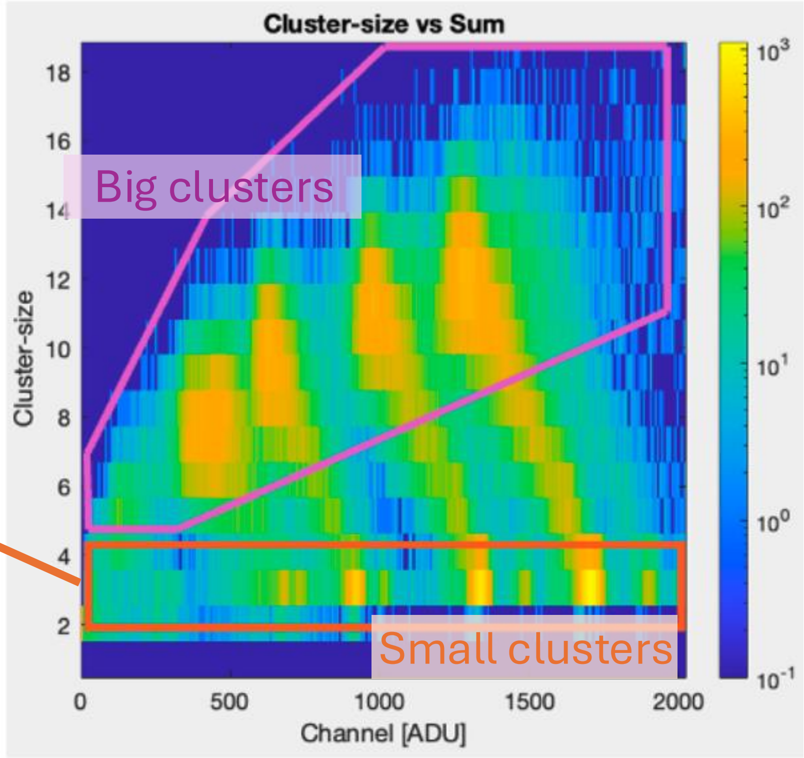

Plasmas for Astrophysics Nuclear Decay Observation and Radiation for Archaeometry

Multi-parameteric energy calibration

Istituto Nazionale di Fisica Nucleare
Laboratori Nazionali del Sud

The energy calibration of the two classes is performed in different ways.

Small clusters → linear energy calibration

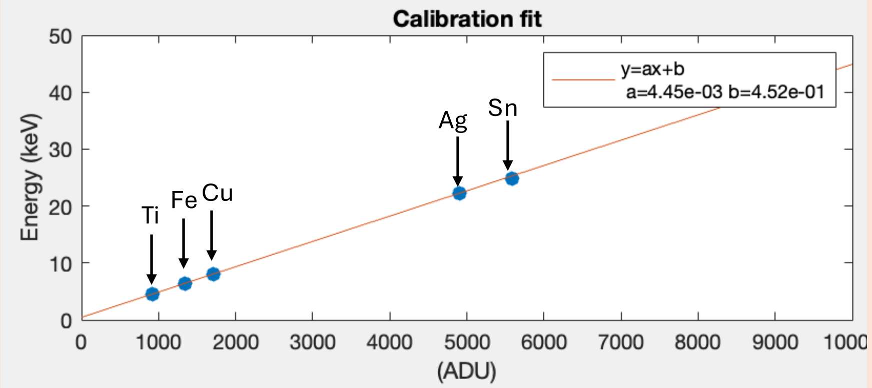

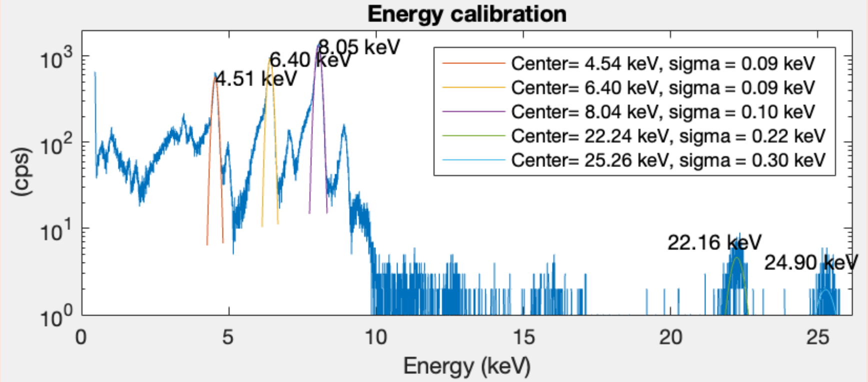

FWHM=236 eV @ 8 keV

Big clusters → multi-parametric energy calibration

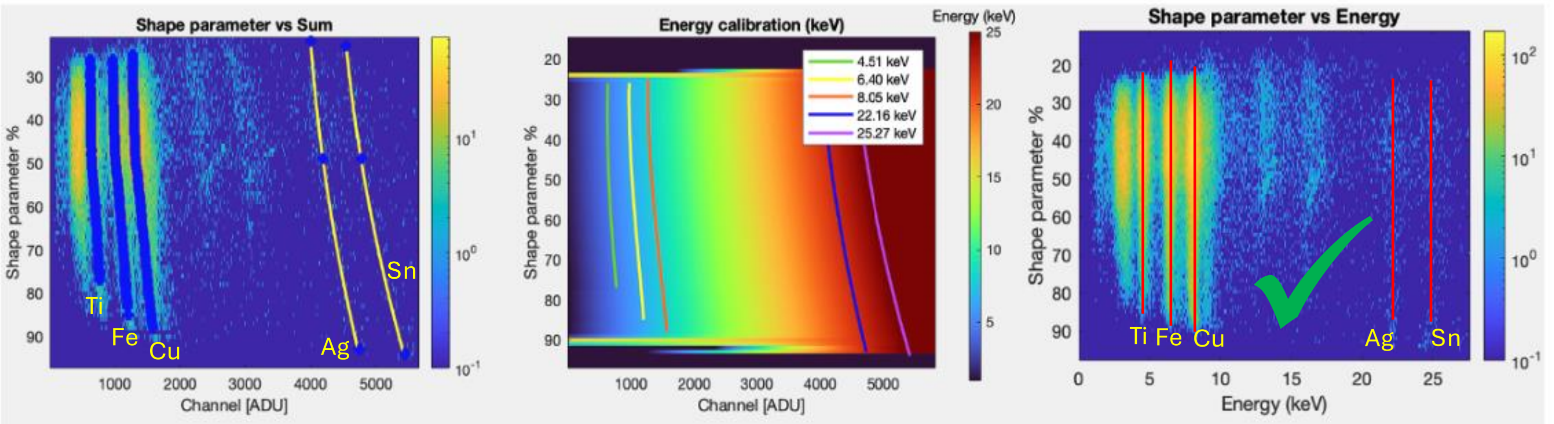

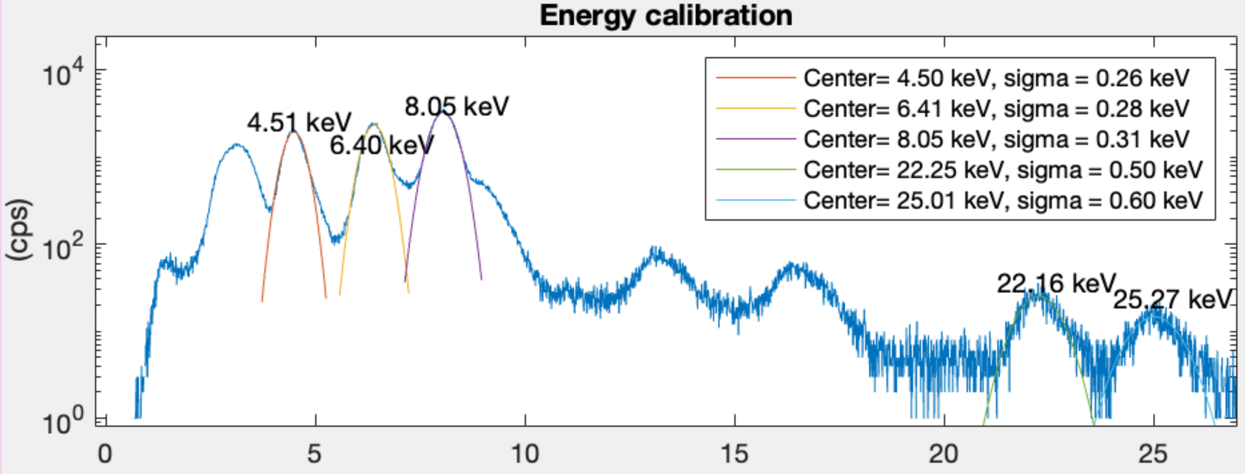

FWHM=730 eV @ 8 keV

Quantum efficiency calibration

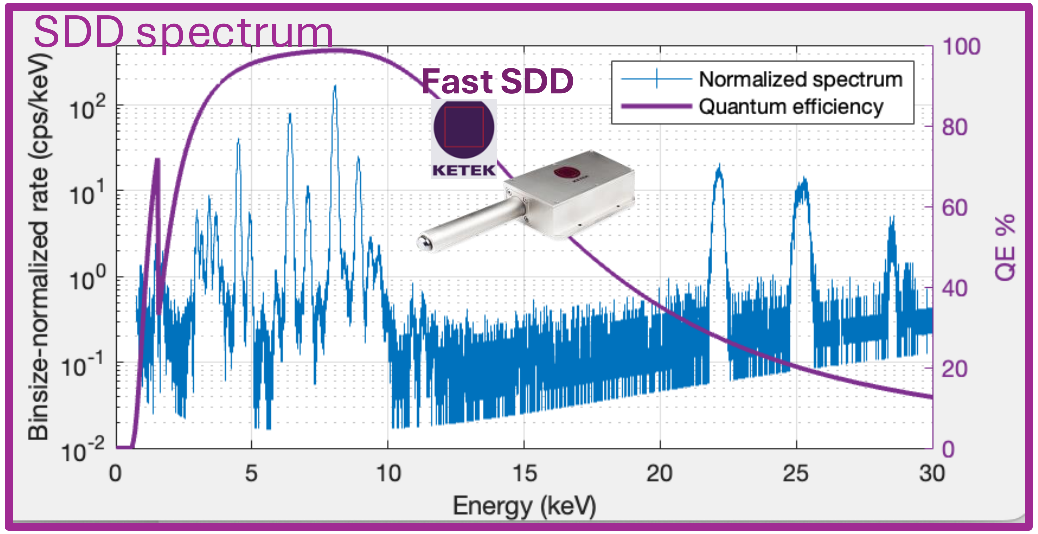

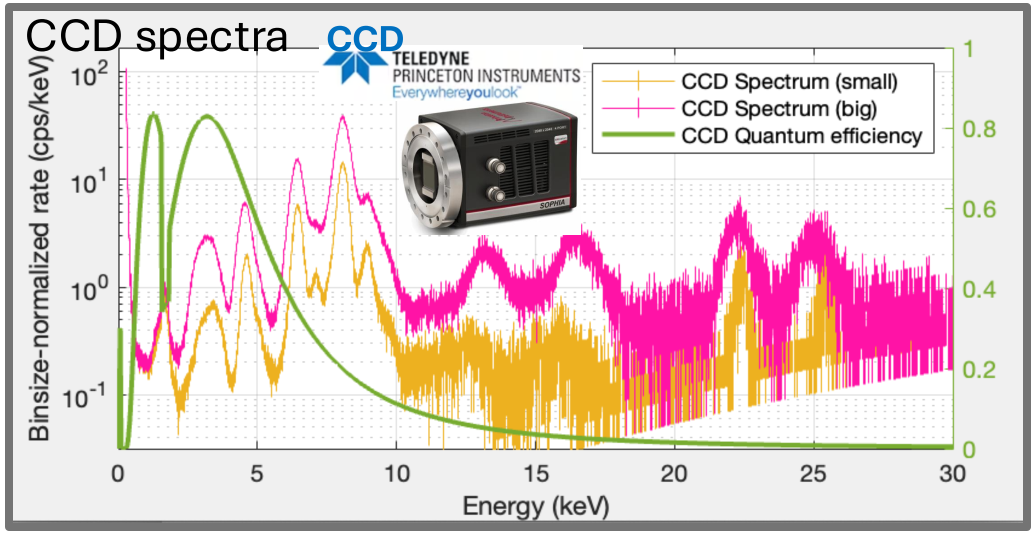

It is possible to define the **effective efficiency of the SPhC algorithm**, intended as the probability P(E) for a detected event to be recognized and classified.

Moreover, such definition can be extended to the **subsamples** having specific features (namely, big and small cluster size).

Quantum efficiency calibration

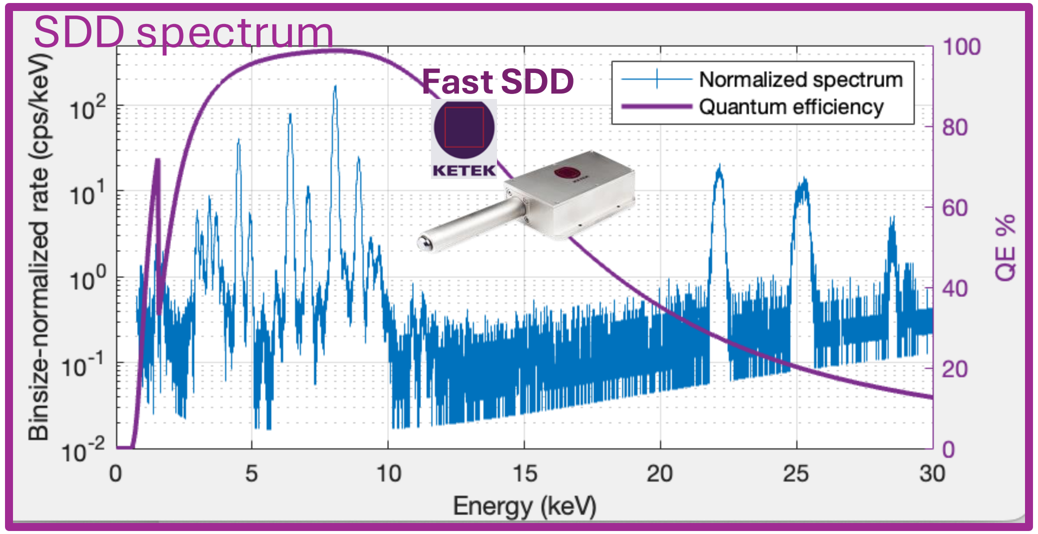

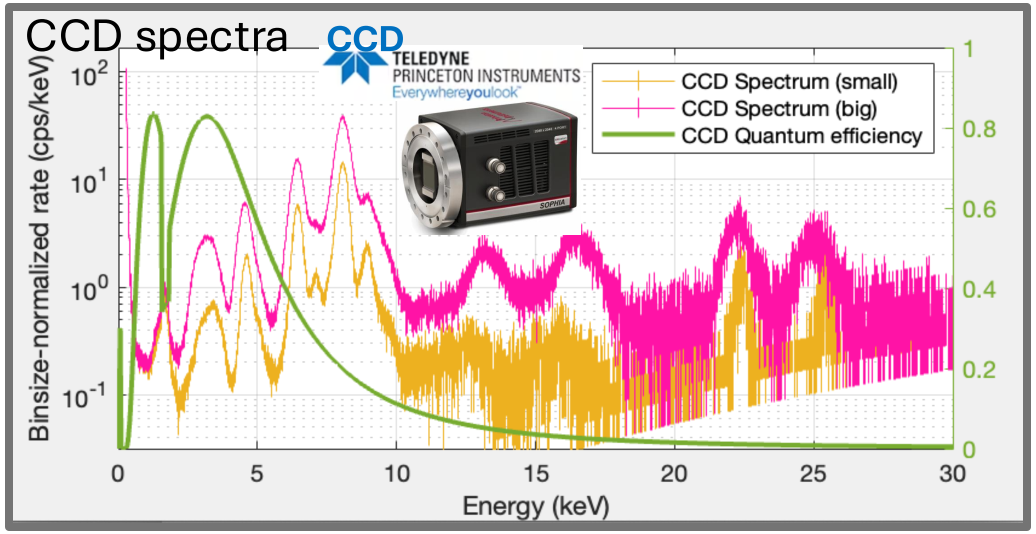

It is possible to define the **effective efficiency of the SPhC algorithm**, intended as the probability P(E) for a detected event to be recognized and classified.

Moreover, such definition can be extended to the **subsamples** having specific features (namely, big and small cluster size).

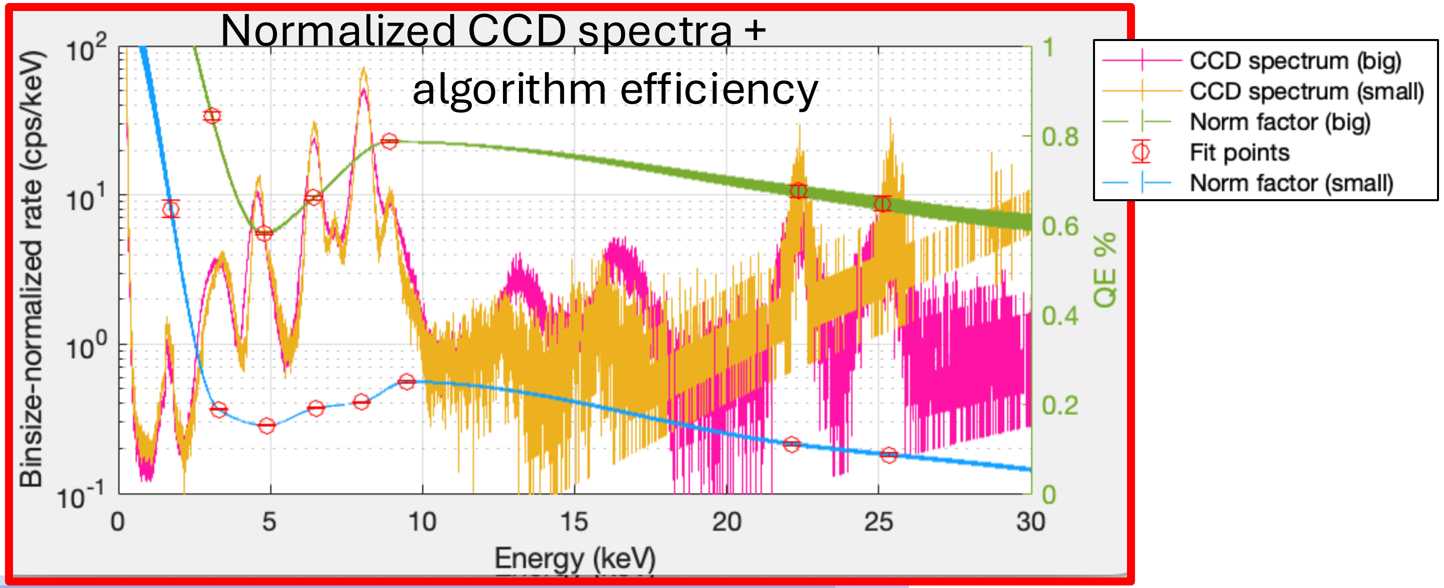

Space and time resolved application

- Introduction: X-ray imaging on ECR plasmas
- Single-photon-counting technique on CCD detectors
- Energy calibration by XRF test-bench
- **ECR plasma imaging at Atomki laboratory: Space and time resolved application**

Experimental campaign
November 3-16, 2024
at Atomki, Debrecen

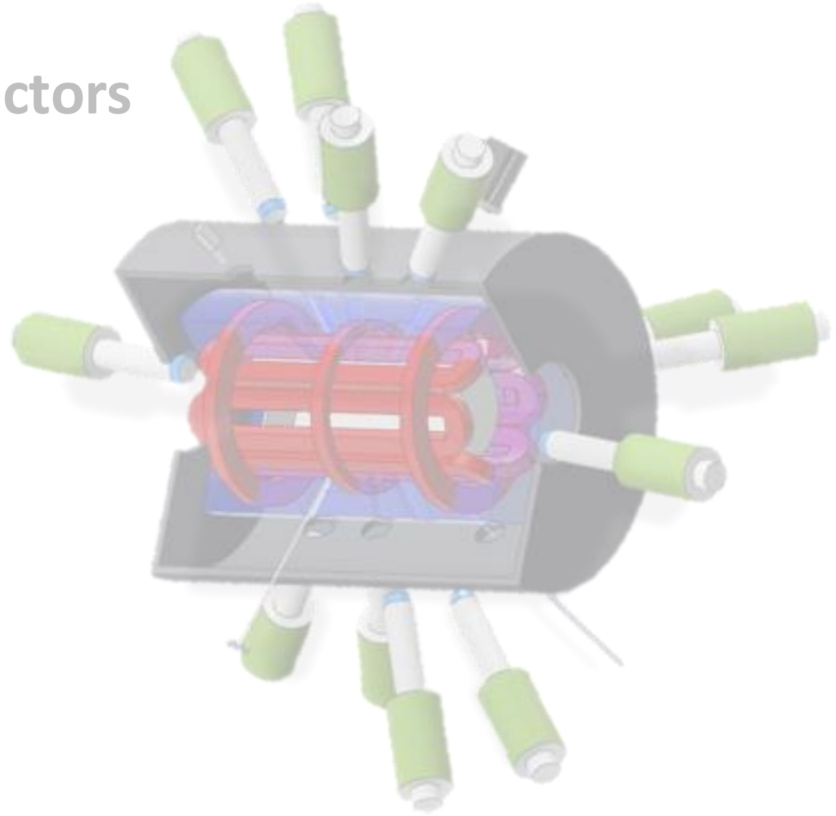

ECR plasma physics investigation: gas mixing effects

PHYSICAL REVIEW ACCELERATORS AND BEAMS **20**, 013402 (2017)

Numerical simulations of gas mixing effect in electron cyclotron resonance ion sources

V. Mironov,* S. Bogomolov, A. Bondarchenko, A. Efremov, and V. Loginov
Joint Institute for Nuclear Research, Flerov Laboratory of Nuclear Reactions, Dubna, Moscow Region 141980, Russia

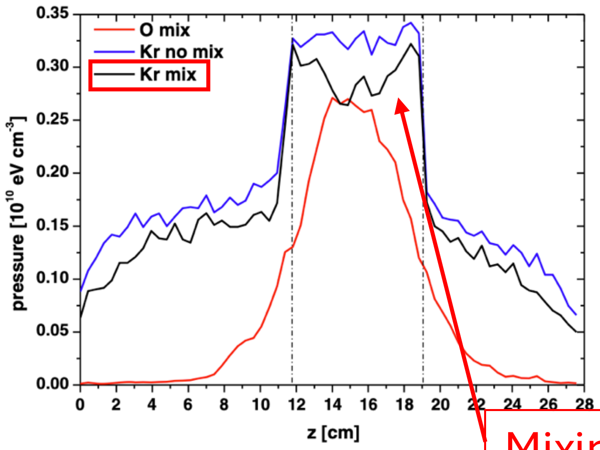

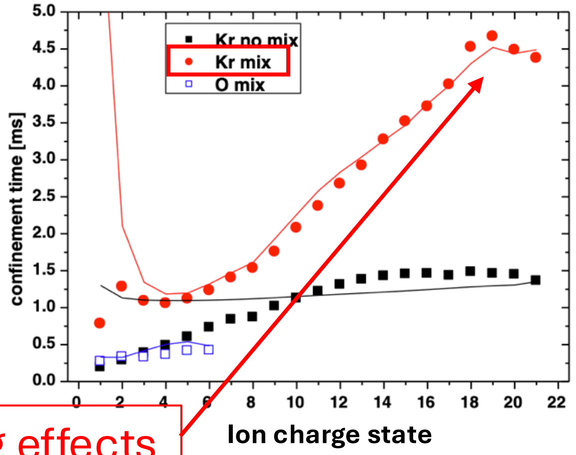

Mixing effects

FIG. 8. Ion pressure profiles along the source z axis: pressure of the oxygen ions (red line), pressure of the krypton ions at Kr = 95%, O = 5% (black line), and pressure of the krypton ions at Kr = 100% (blue line).

FIG. 11. Confinement times of krypton ions for the krypton plasma (black squares) and in the mix with oxygen (red circles) as a function of the ion charge state. Confinement times of oxygen ions in the mix are shown as the open blue squares. The Rognlien-Cutler fits are shown as the lines.

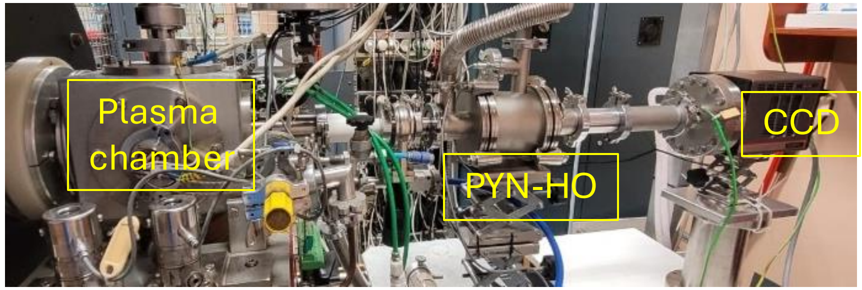

Mixing two gases in an electron cyclotron resonance ion source (ECRIS) is a **common technique** to **increase currents** of the highest charge states of a heavier element.

Gas mixing plasma imaging

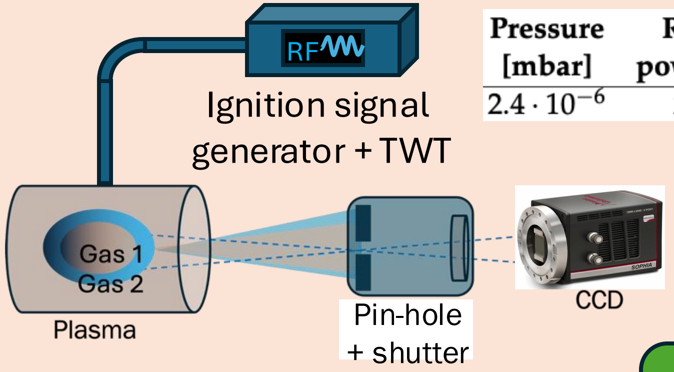

Pressure [mbar]	RF net power [W]	B_{min}/B_{ECR}
$2.4 \cdot 10^{-6}$	201.2	0.77

Multielemental plasma characterization → Confinement morphology investigation

First time direct observation

Plasma imaging at Atomki lab: gas mixing

Gas mixing distribution investigation

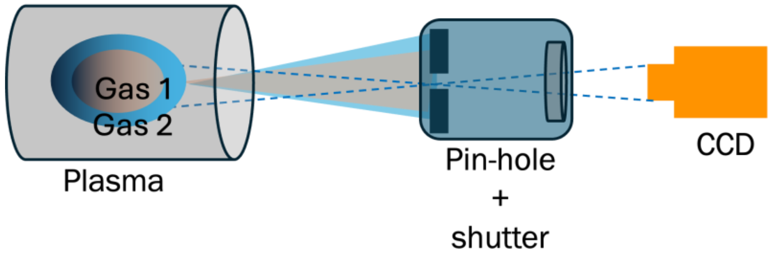

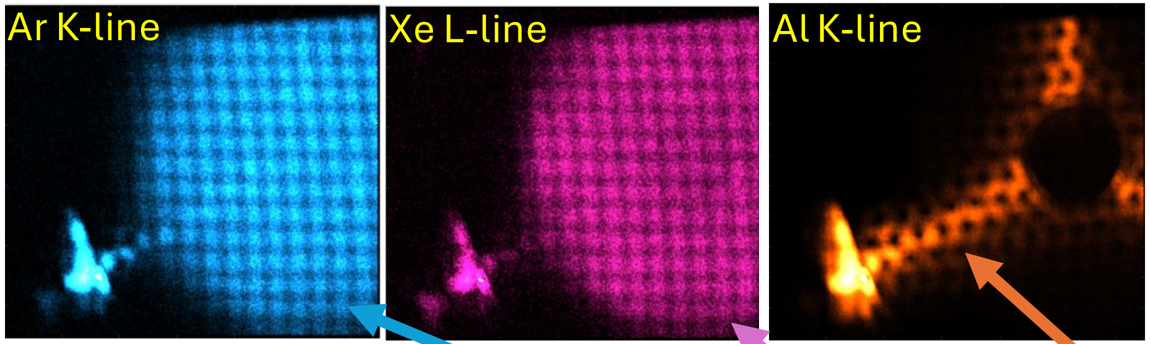

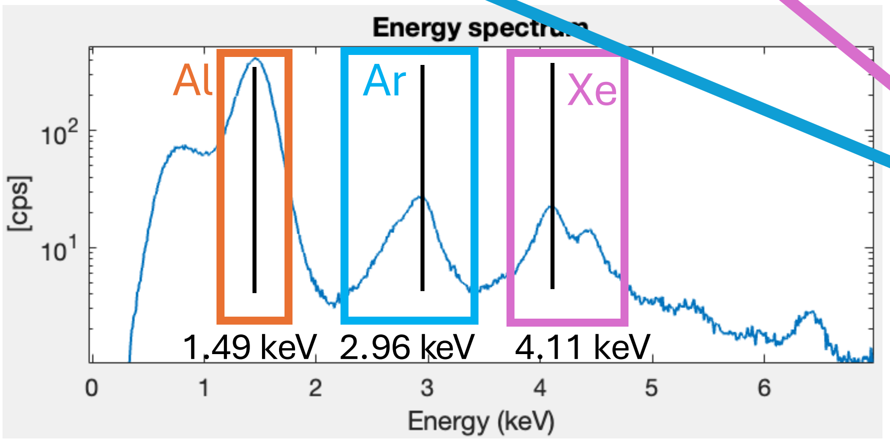

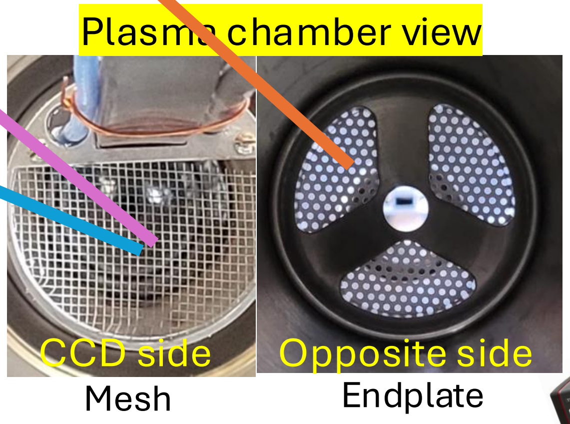

Investigation of ECR plasma confinement in Ar+Xe gas-mixing configuration

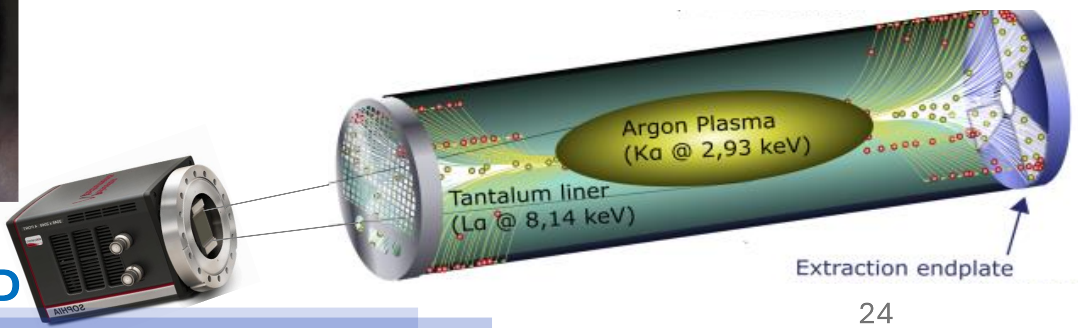

Plasma imaging at Atomki lab: gas mixing

Gas mixing distribution investigation

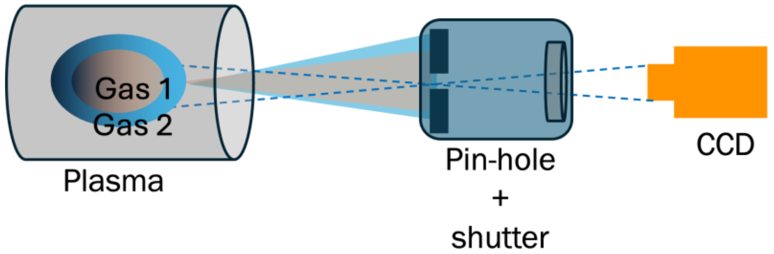

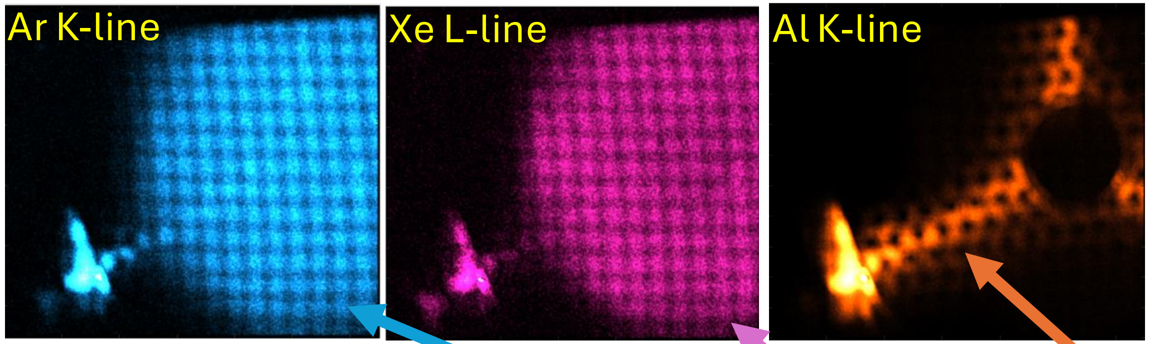

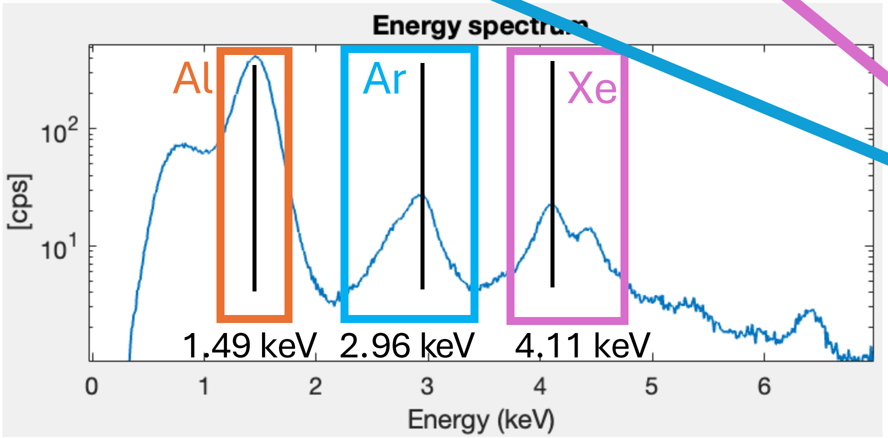

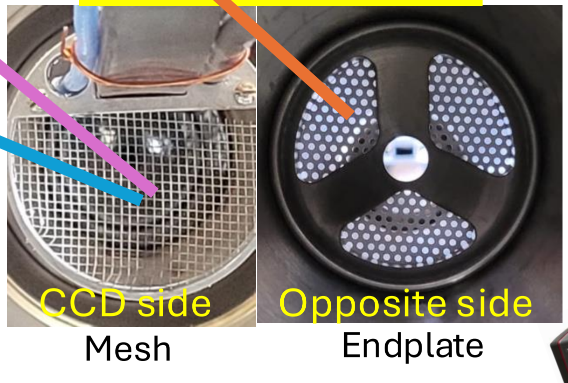

Plasma confinement structure

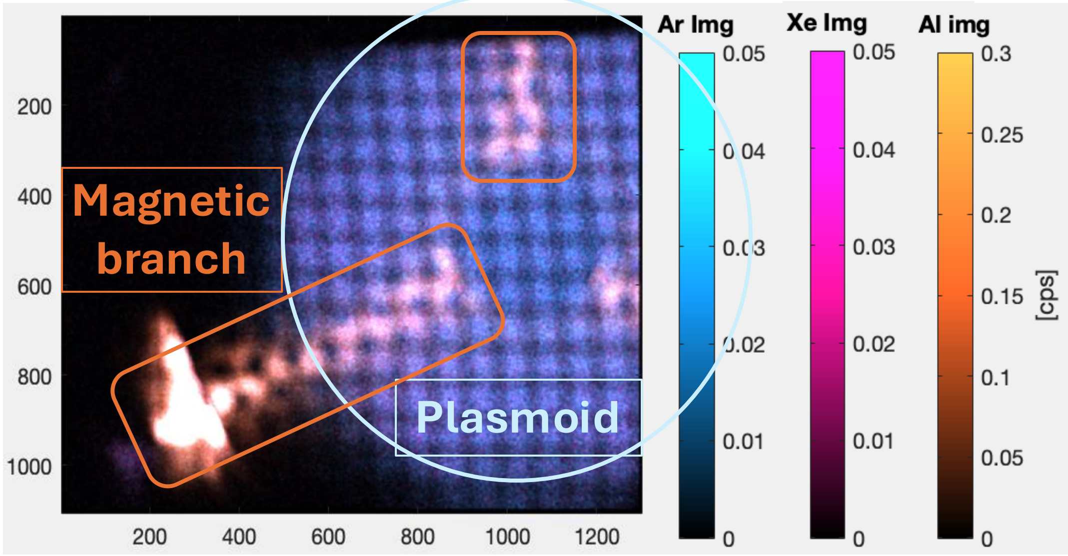

Investigation of ECR plasma confinement in Ar+Xe gas-mixing configuration

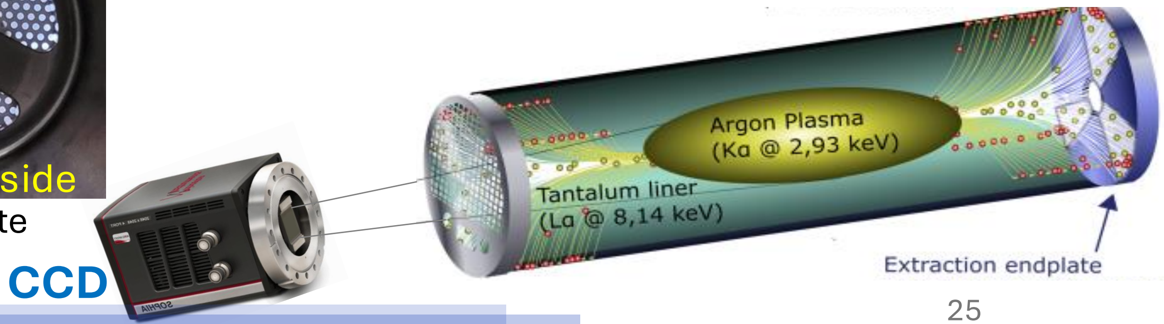

Plasma imaging at Atomki lab: gas mixing

Gas mixing distribution investigation

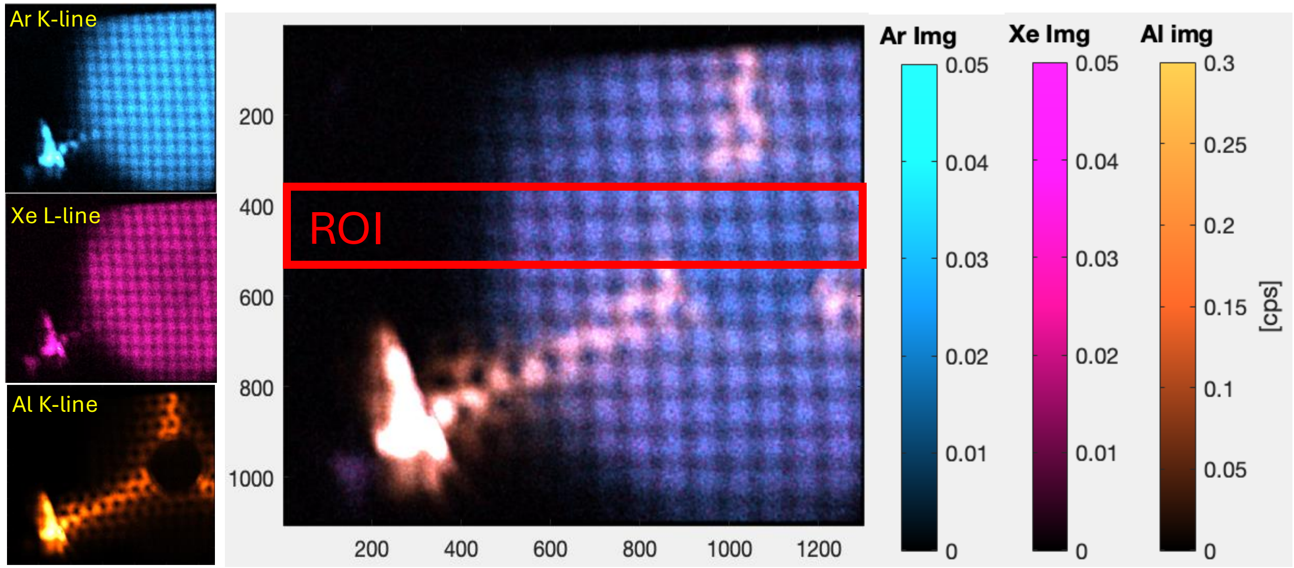

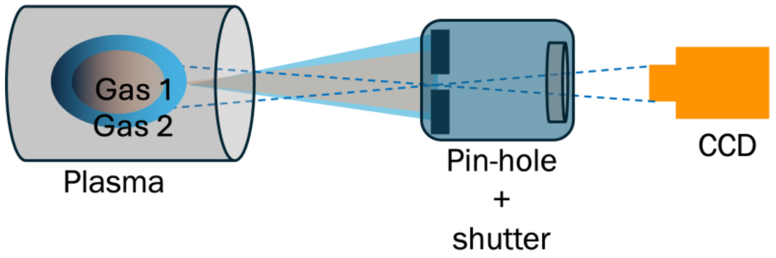

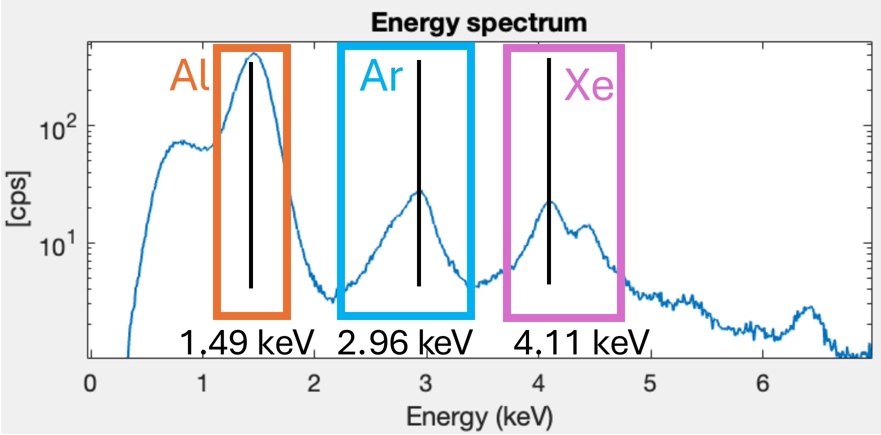

The **morphology** of plasma confinement changes in the **gas-mixed** case

Plasma imaging at Atomki lab: gas mixing

Gas mixing distribution investigation

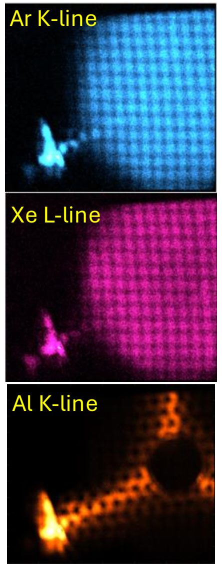

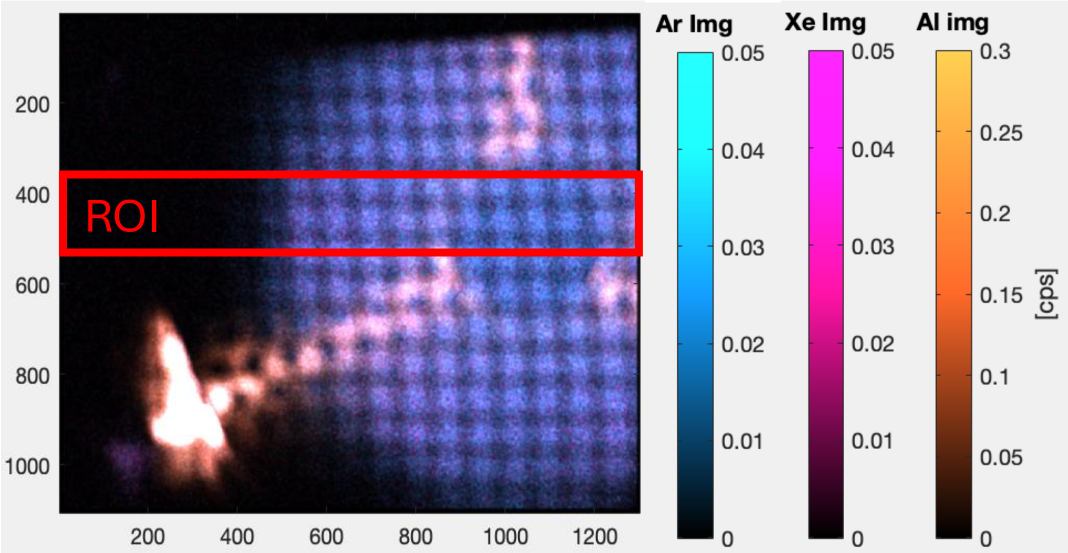

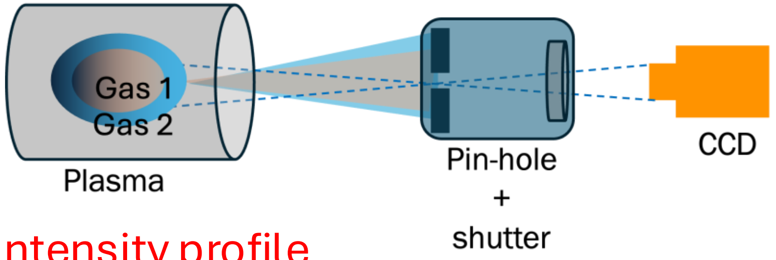

X-intensity profile

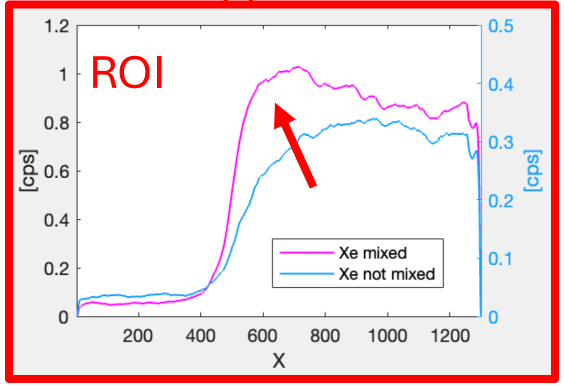

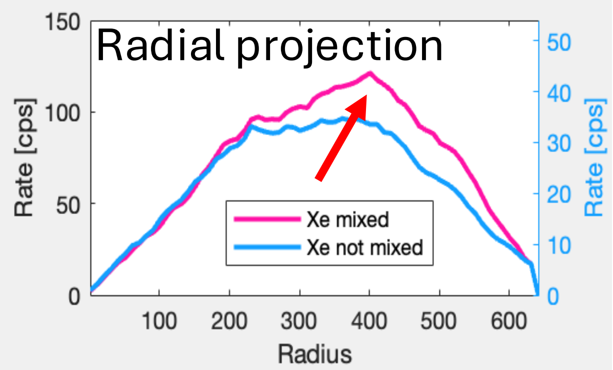

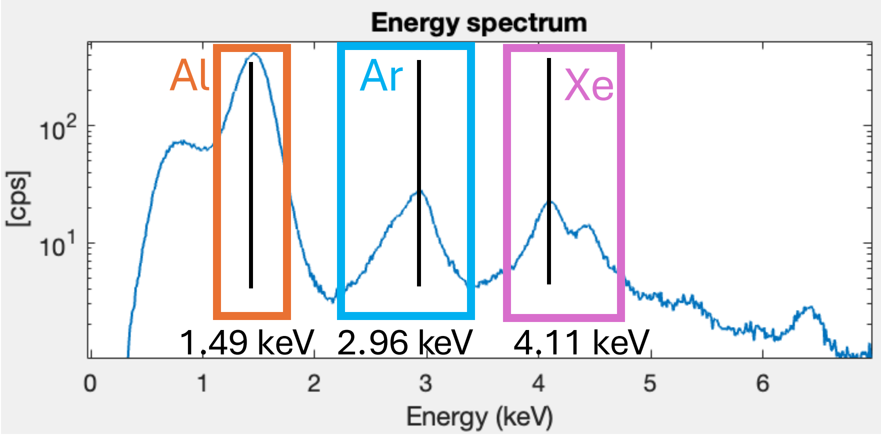

The **morphology** of plasma confinement changes in the **gas-mixed** case

Plasma imaging at Atomki lab: gas mixing

Gas mixing distribution investigation

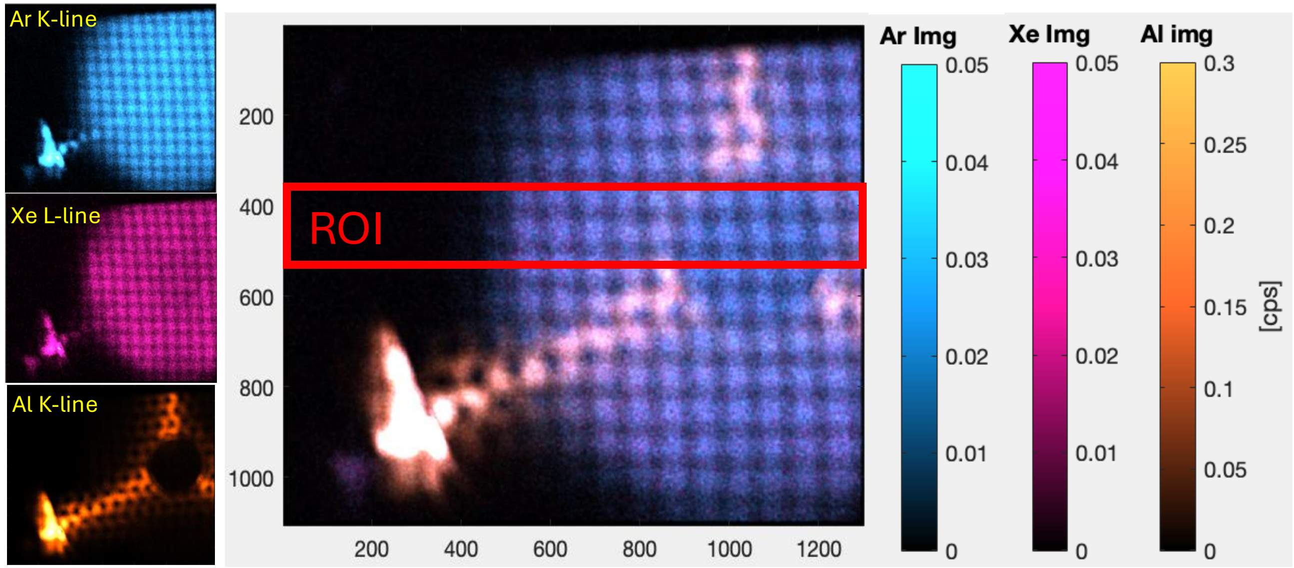

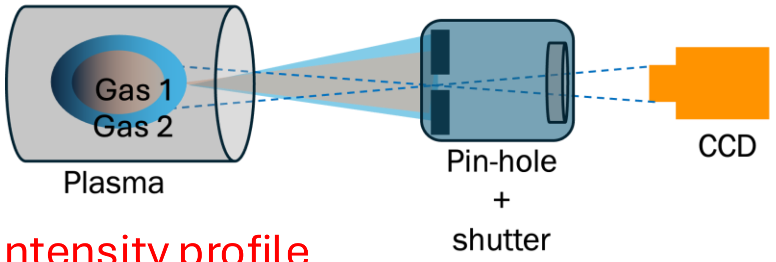

X-intensity profile

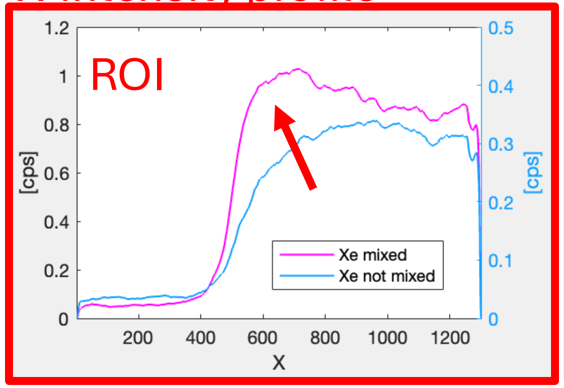

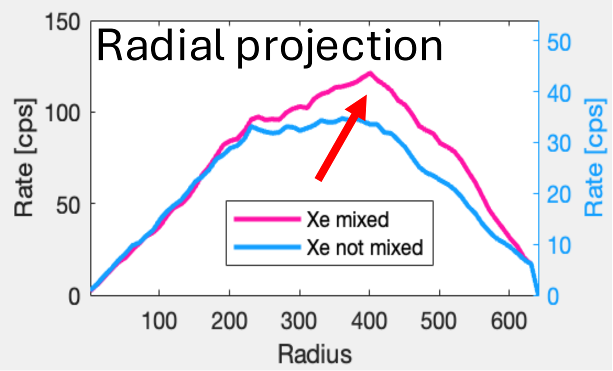

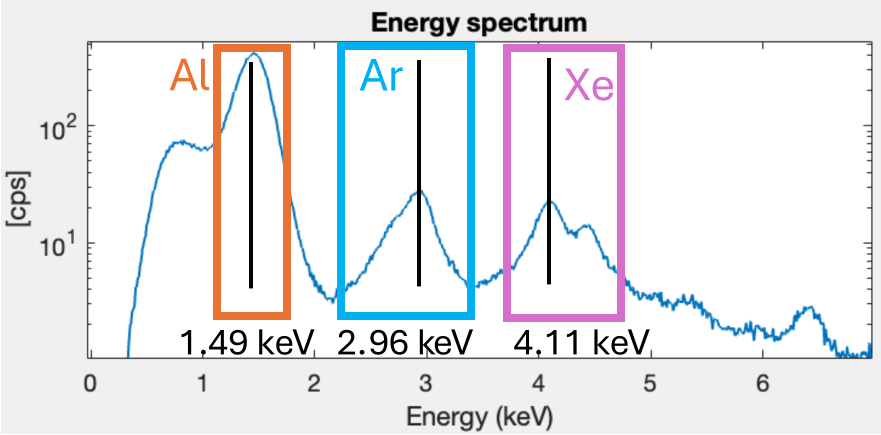

Azimuthal projection

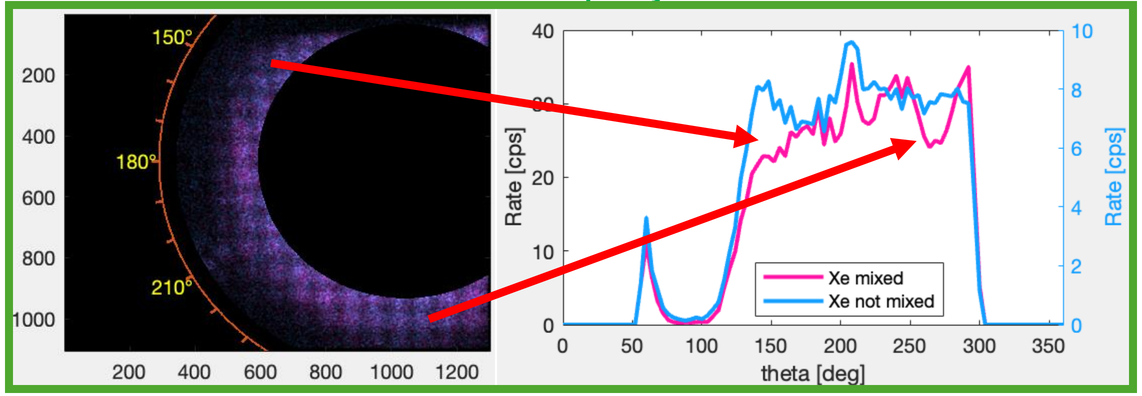

The **morphology** of plasma confinement changes in the **gas-mixed** case

ECR plasma physics investigation: Afterglow plasma decay

Plasma Phys. Control. Fusion **67** (2025) 035012 (10pp)

Ion confinement and temperature in minimum-B electron cyclotron resonance ion source plasmas

O Tarvainen[1,*], V Toivanen[2], O Timonen[2], R Kronholm[2] and H Koivisto[2]

[1] UK Research and Innovation, STFC Rutherford Appleton Laboratory, Harwell Campus, Didcot OX11 0QX, United Kingdom
[2] Accelerator Laboratory, Department of Physics, University of Jyväskylä, FI-40014 Jyväskylä, Finland

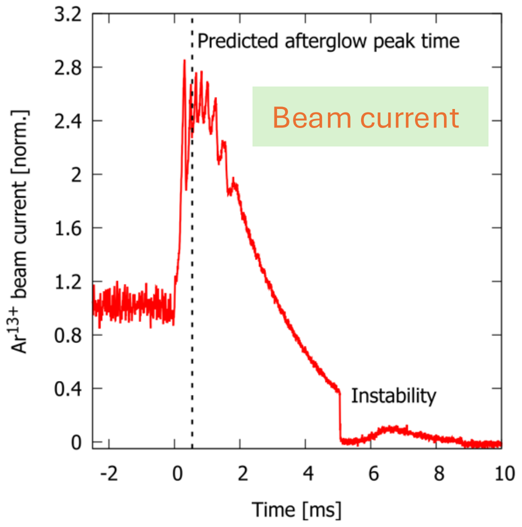

Figure 4. A representative example of Ar^{13+} afterglow peak measured with the JYFL 14 GHz ECRIS with 1 Hz microwave pulse repetition rate and 50% duty factor. The beam current is normalised to the steady-state average value at $t < 0$. The microwave power is switched off at $t = 0$. The predicted afterglow peak time is shown with a vertical dashed line.

The **ion current** extraction **decays** in the time scale of **10 ms.**

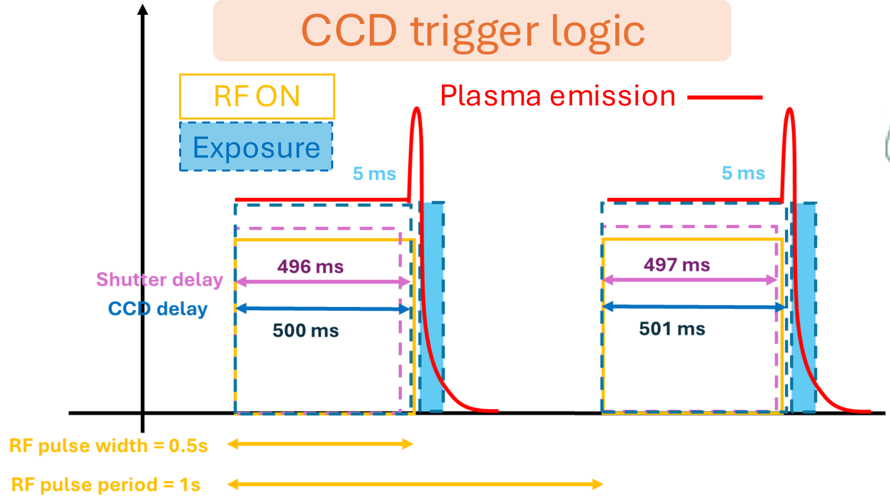

Plasma switch-off decay transient investigation

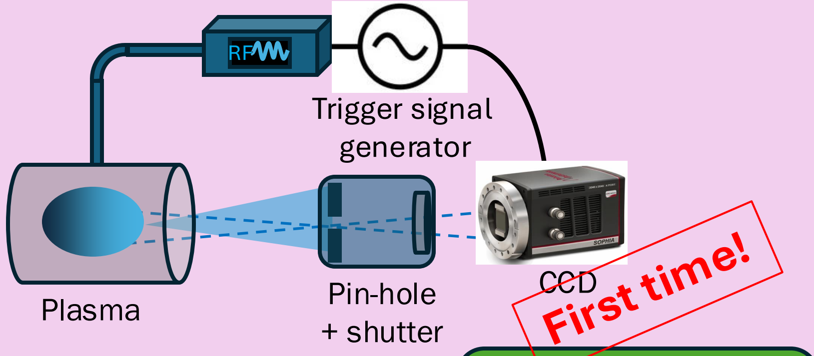

Pressure [mbar]	RF net power [W]	B_{min}/B_{ECR}
$2.4 \cdot 10^{-6}$	201.2	0.77

Time-resolved plasma imaging

Plasmas for Astrophysics Nuclear Decay Observation and Radiation for Archaeometry

Plasma imaging at Atomki lab: decay transient

INFN LNS Istituto Nazionale di Fisica Nucleare Laboratori Nazionali del Sud

Plasma decay after RF pumping switch-off

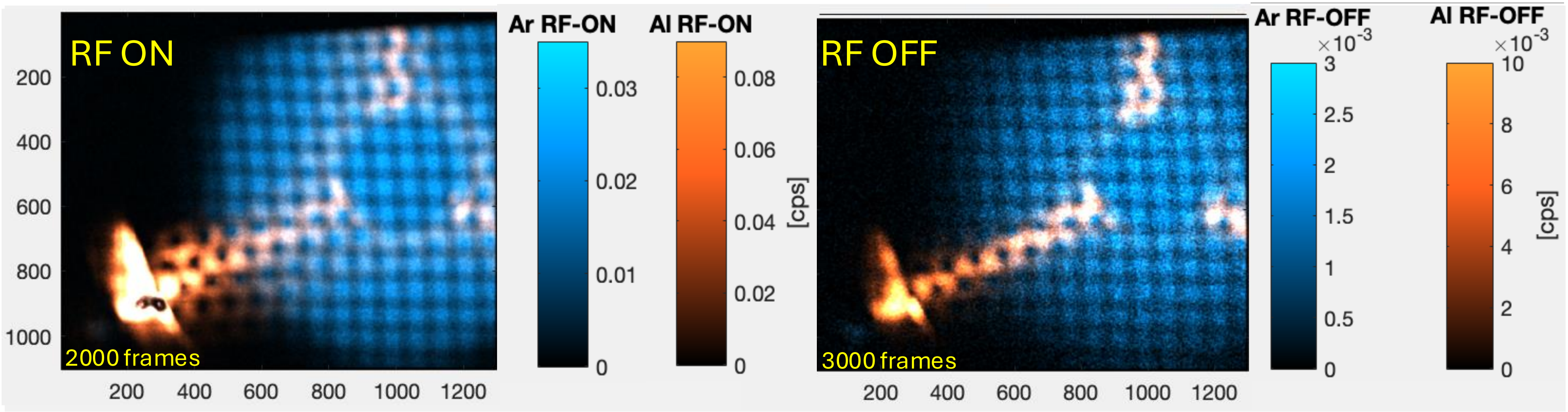

Study of the **morphology** of plasma confinement in the **decay transient** (100 ms) after the RF switch-off.

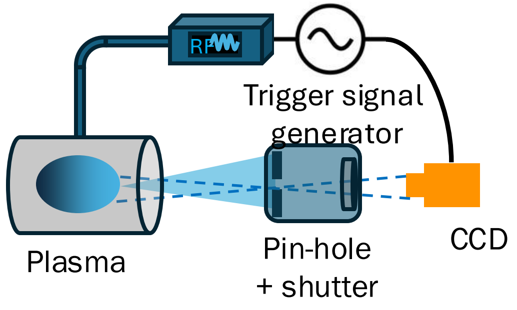

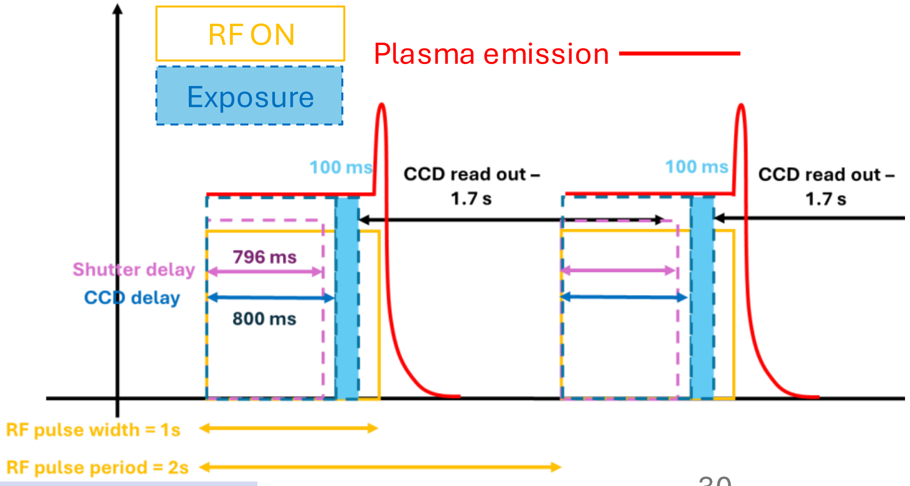

Plasma imaging at Atomki lab: decay transient

Plasma decay after RF pumping switch-off

Study of the **morphology** of plasma confinement in the **decay transient** (100 ms) after the RF switch-off.

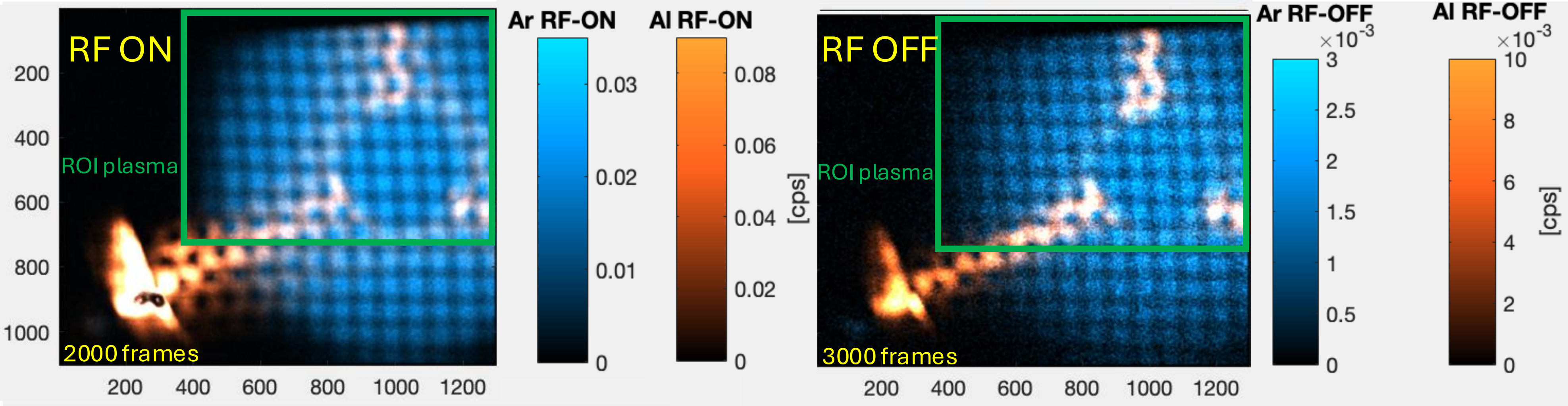

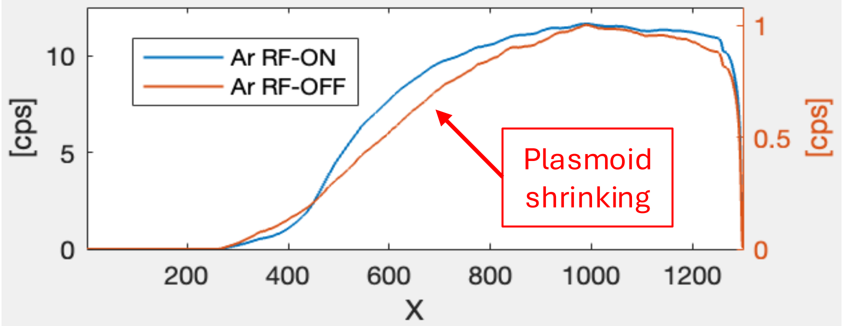

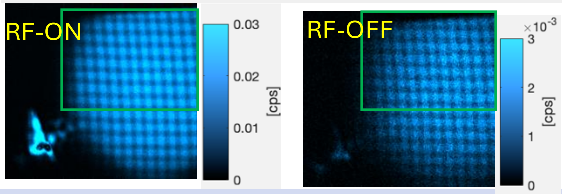

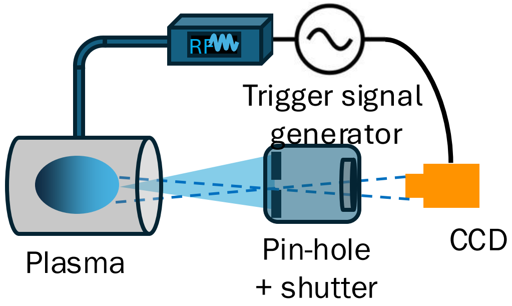

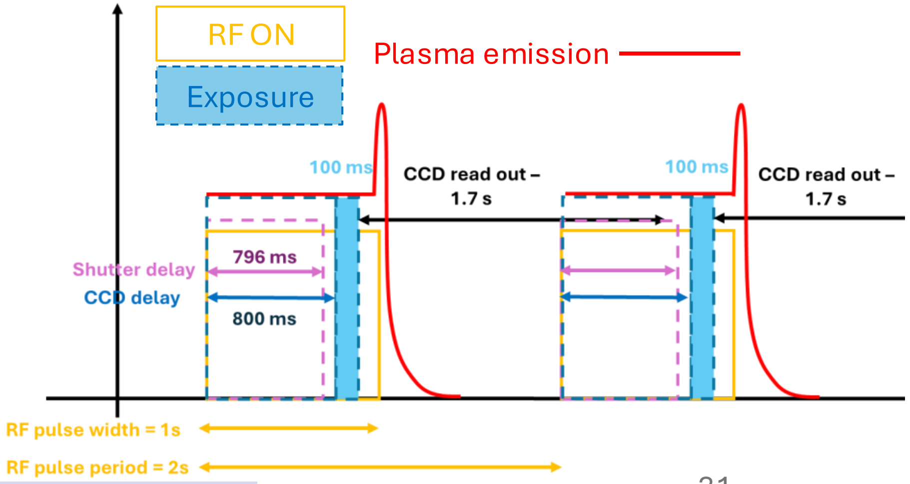

Plasmas for Astrophysics Nuclear Decay Observation and Radiation for Archaeometry

Plasma imaging at Atomki lab: decay transient

INFN LNS
Istituto Nazionale di Fisica Nucleare
Laboratori Nazionali del Sud

Plasma decay after RF pumping switch-off

Study of the **morphology** of plasma confinement in the **decay transient** (100 ms) after the RF switch-off.

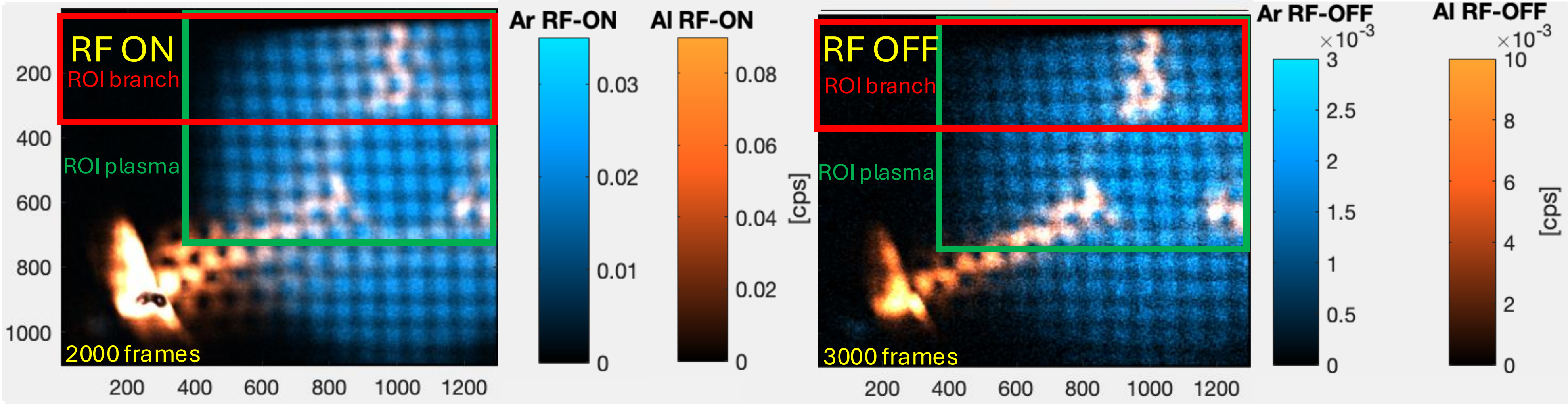

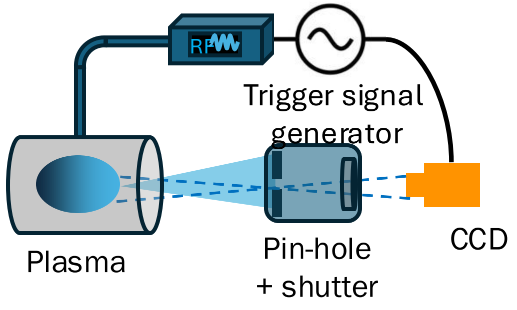

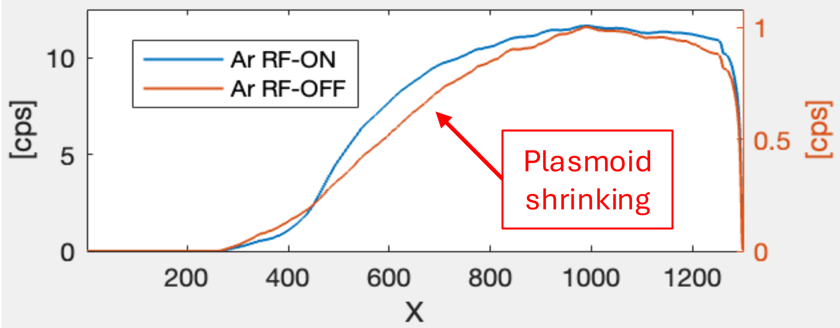

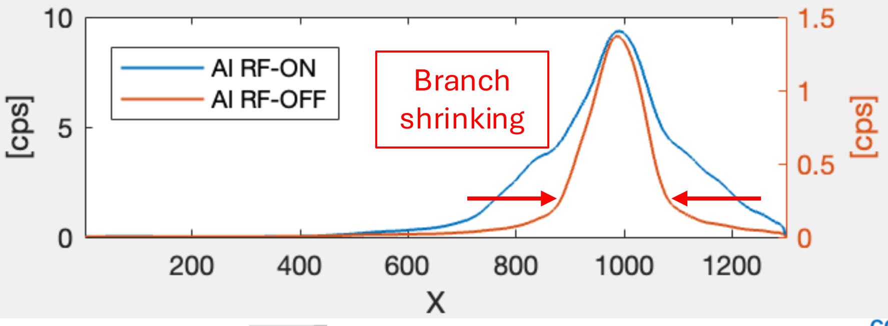

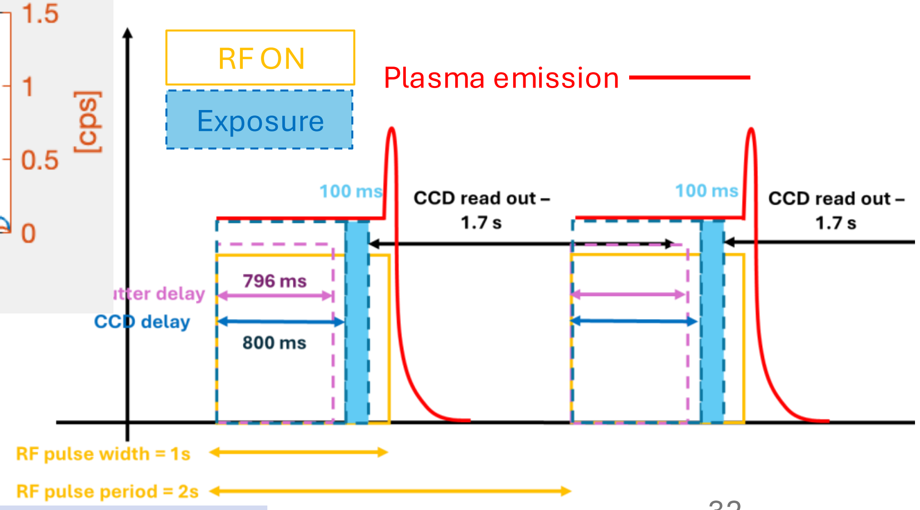

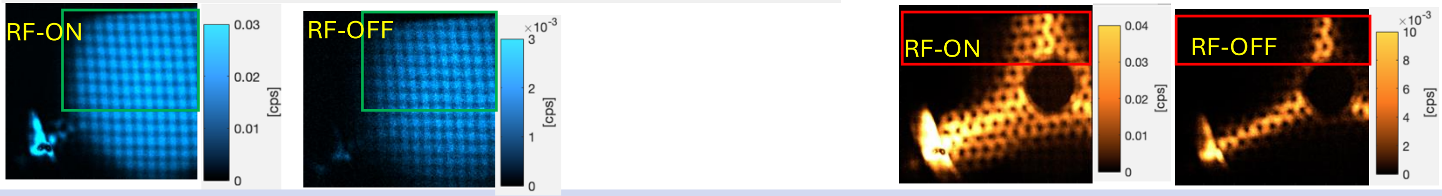

Plasma imaging at Atomki lab: decay transient

Plasma decay time lapse after RF pumping switch-off

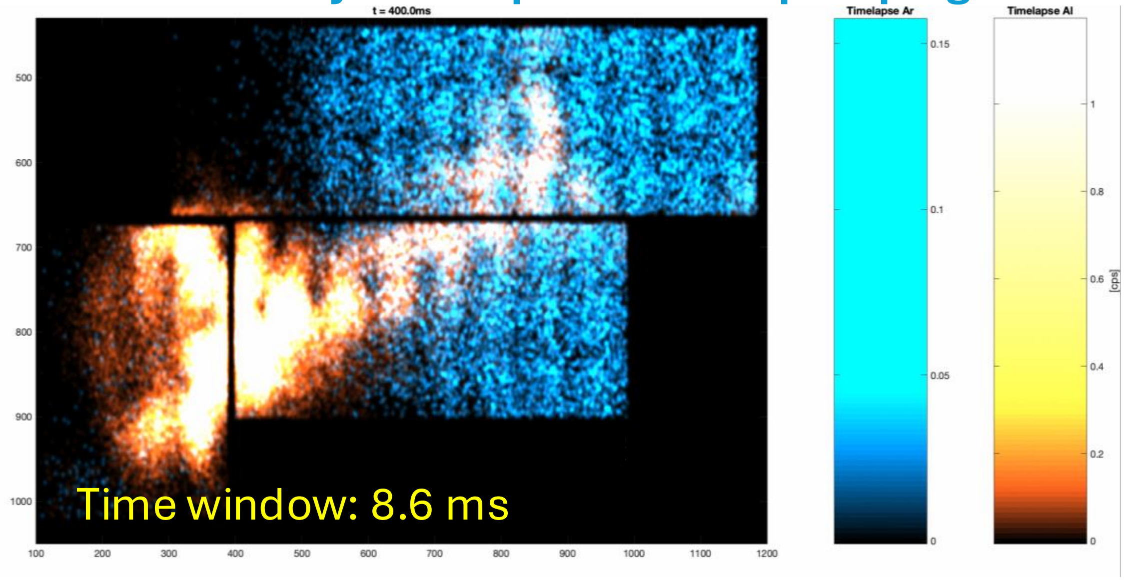

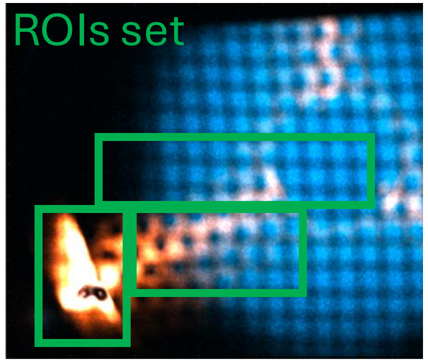

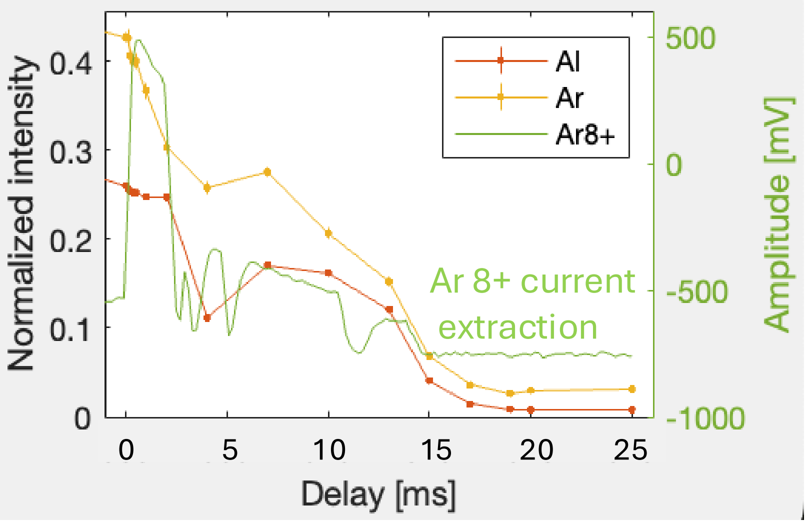

Time evolution of plasma **morphology** in the decay transient.

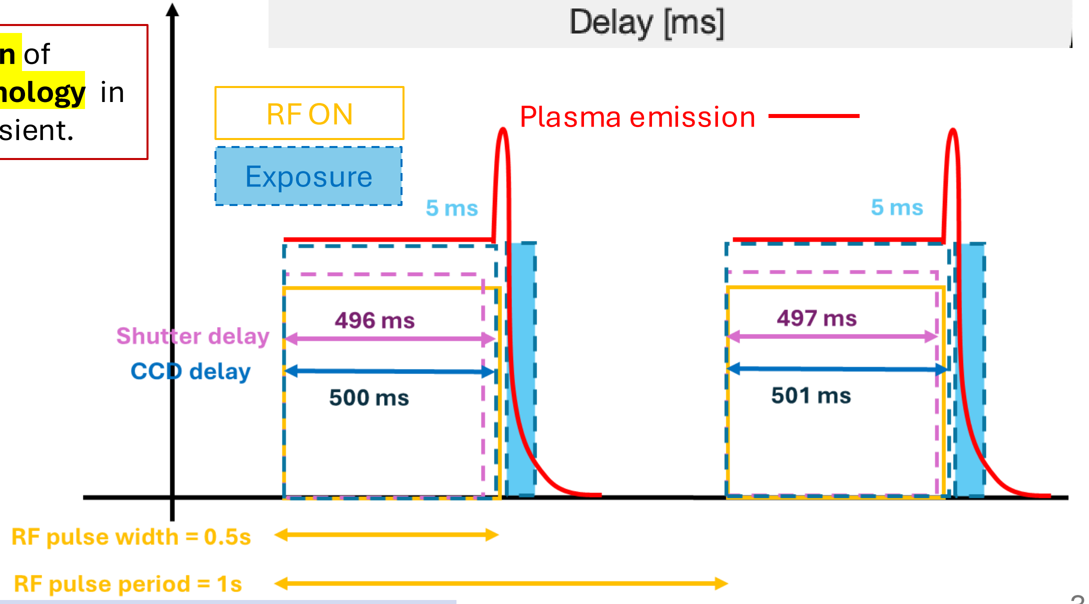

500 frames per time window

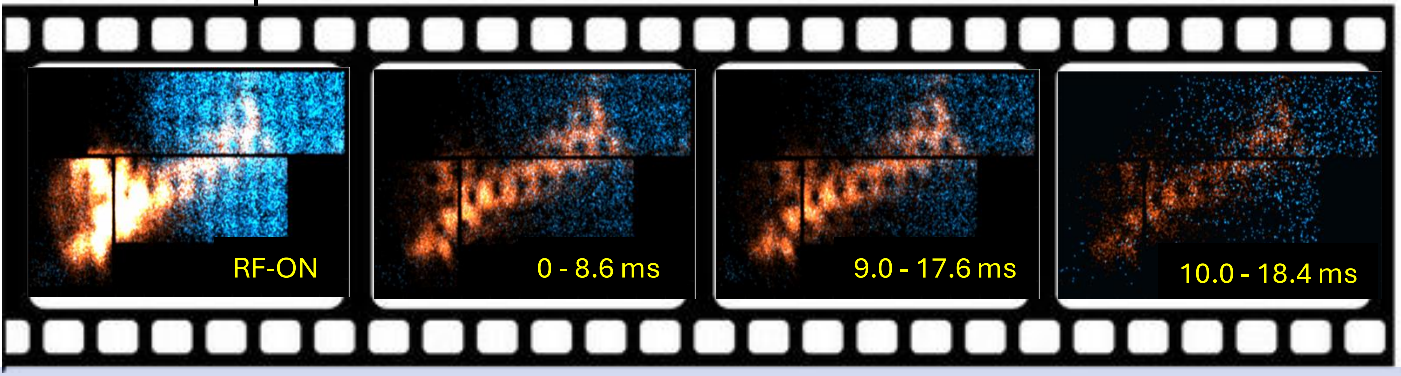

Plasmas for
Astrophysics
Nuclear
Decay
Observation and
Radiation for
Archaeometry

Conclusions

Istituto Nazionale di Fisica Nucleare
Laboratori Nazionali del Sud

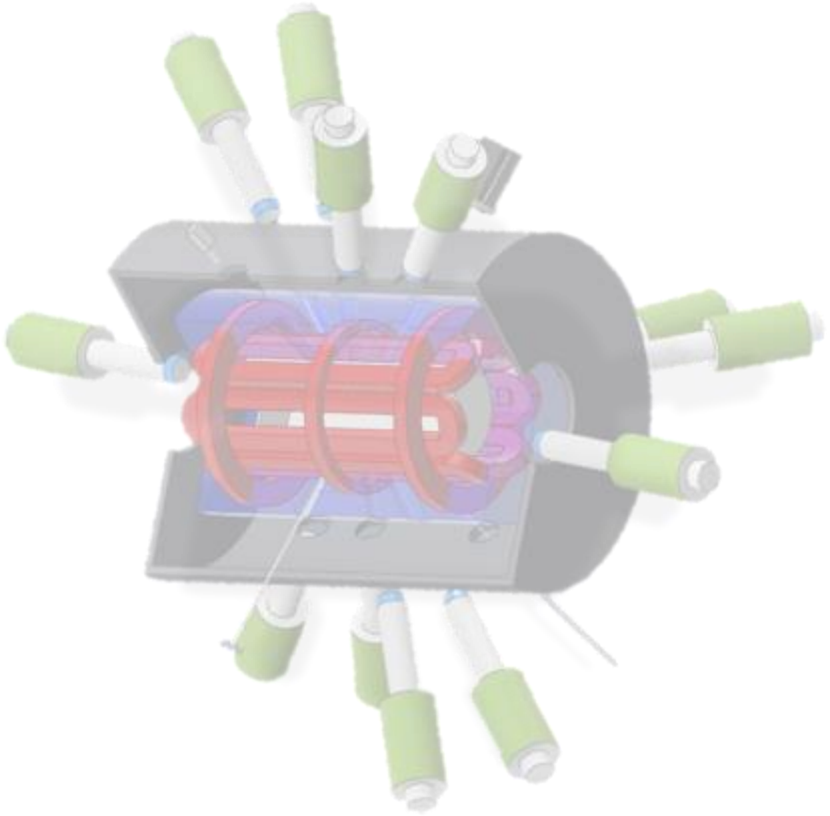

Conclusions

- **CCD characterization**

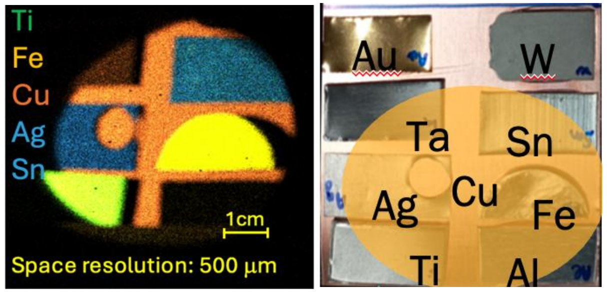

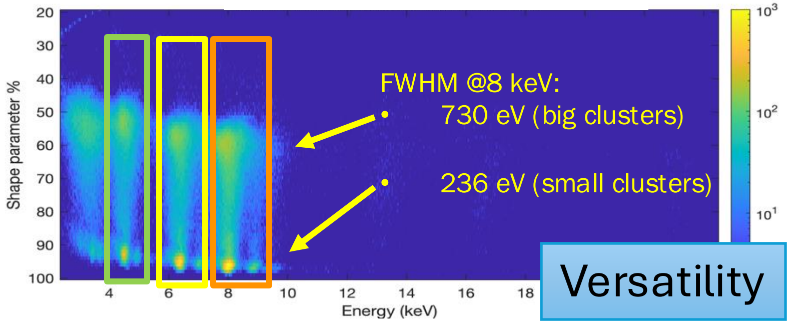

Versatility

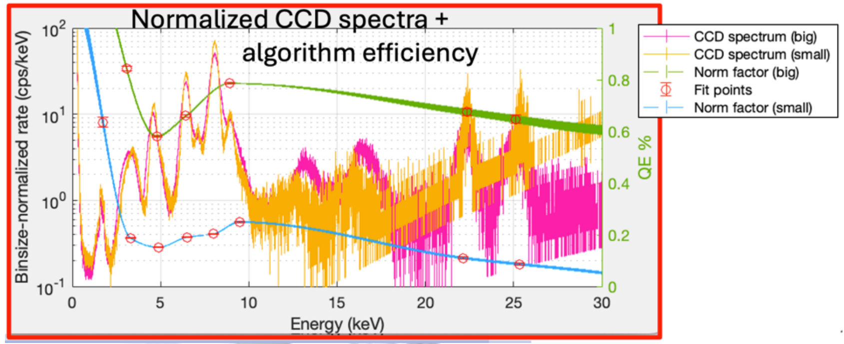

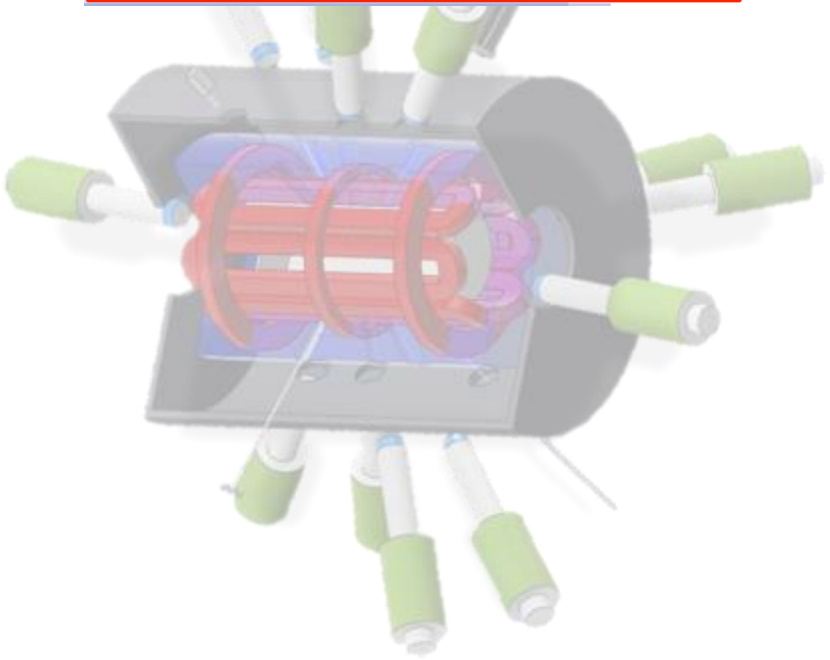

Conclusions

- **CCD characterization**

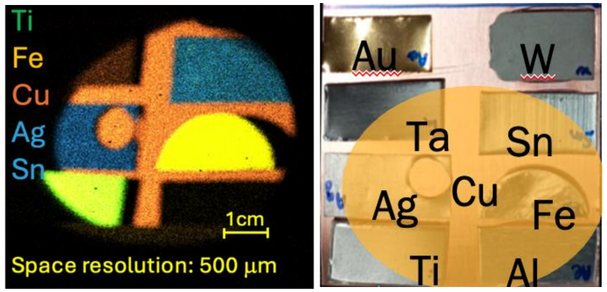

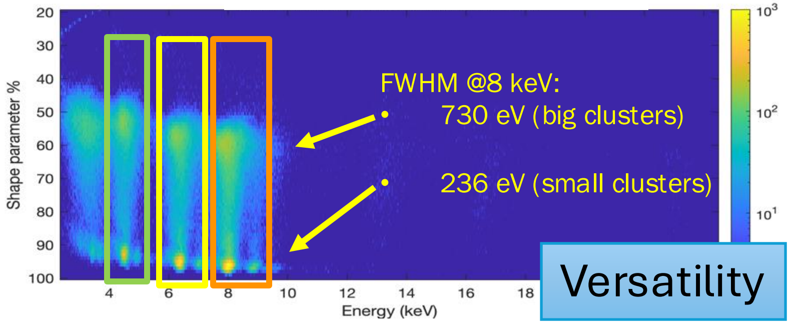

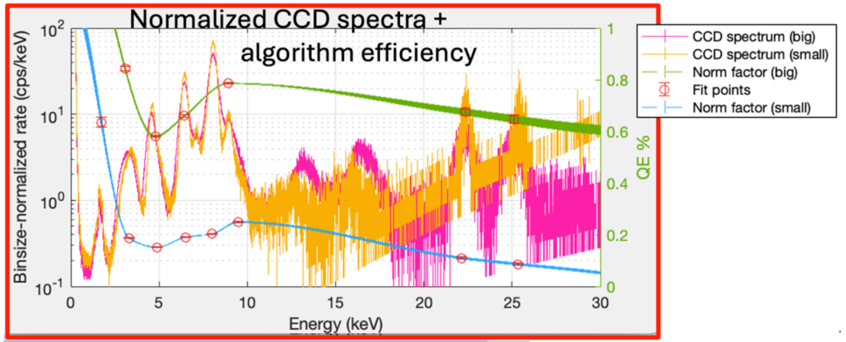

- **Plasma imaging application**

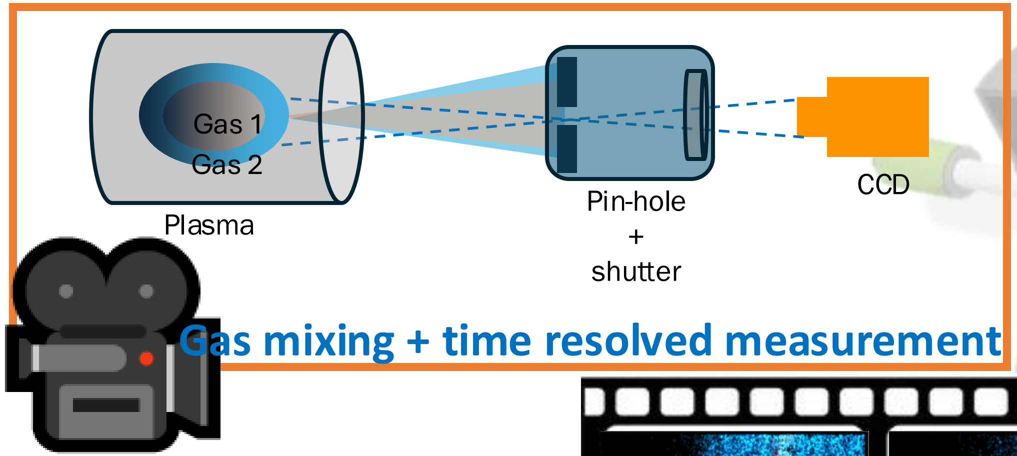

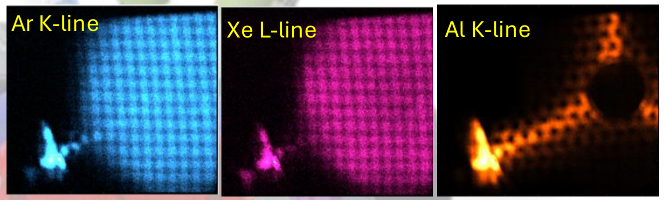

Plasma morphology investigation

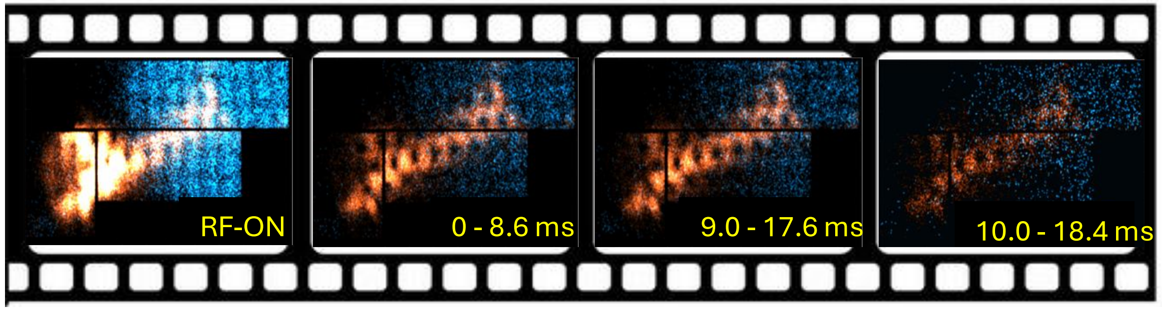

Conclusions

- **CCD characterization**

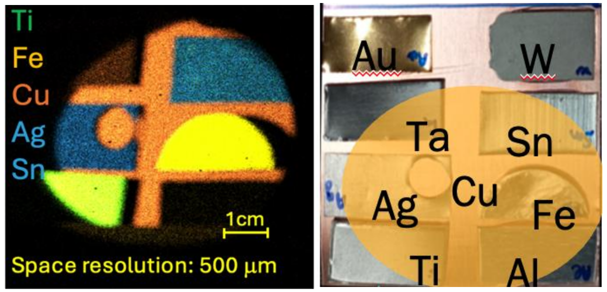

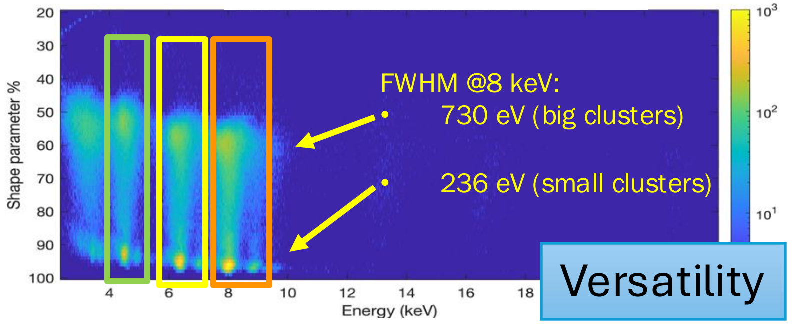

Versatility

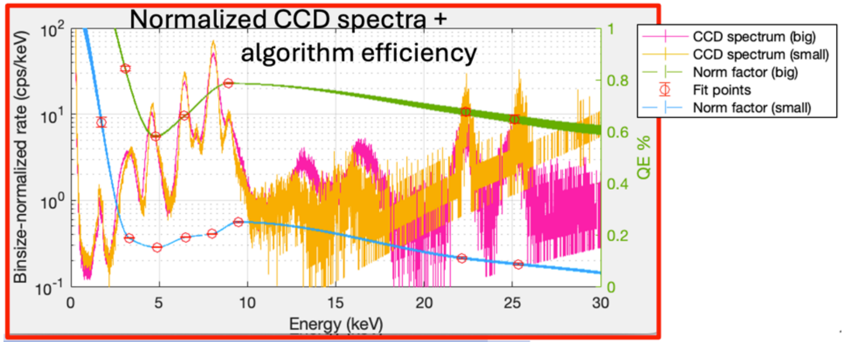

- **Plasma imaging application**

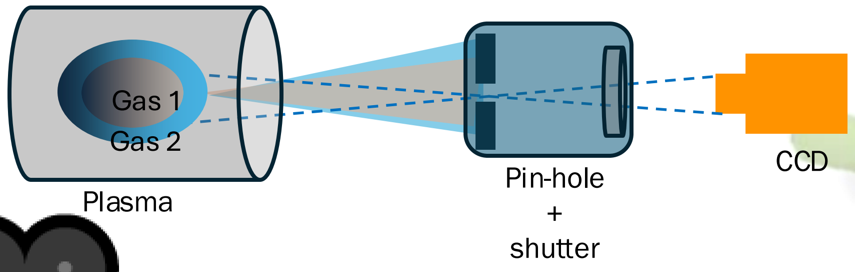

Gas mixing + time resolved measurement

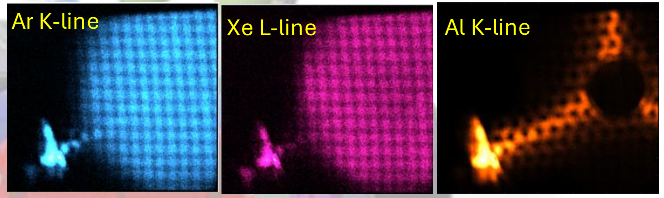

Plasma morphology investigation

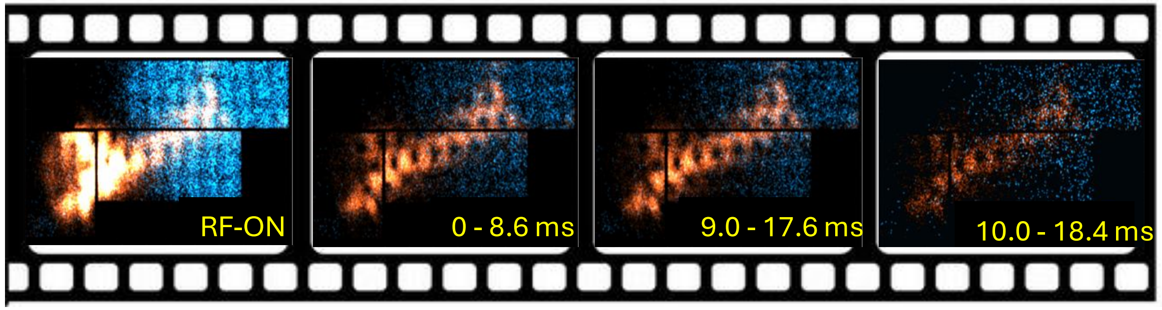

The method allowed to obtain very relevant measurements in the field of ECR plasma.

Interdisciplinary interest: it can be extended to any other X-ray imaging application

Plasmas for Astrophysics Nuclear Decay Observation and Radiation for Archaeometry

Istituto Nazionale di Fisica Nucleare
Laboratori Nazionali del Sud

Thanks for your attention

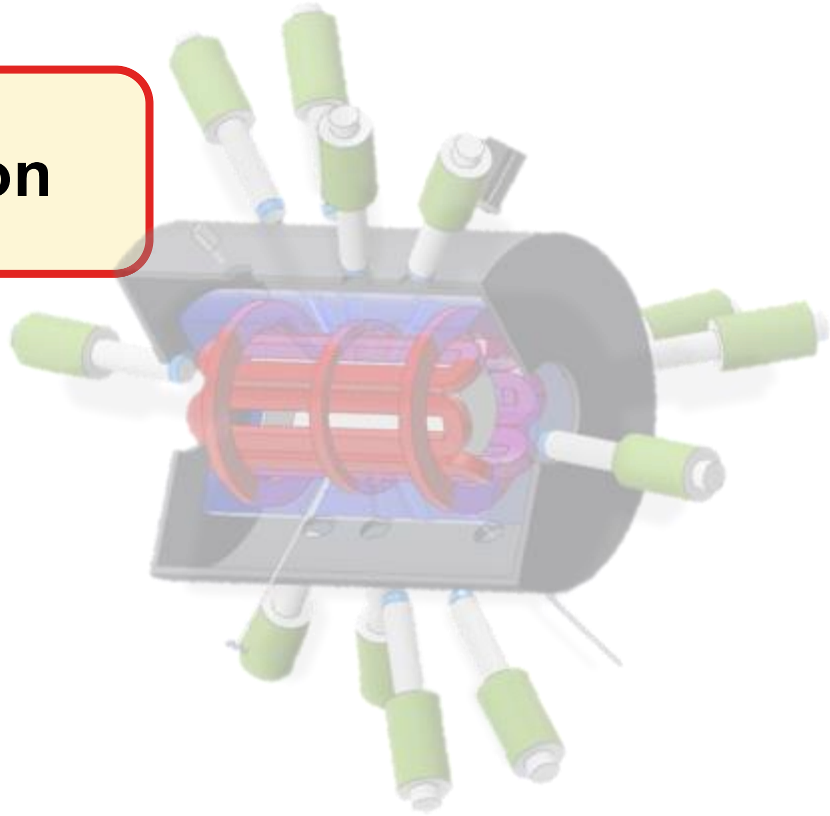

Thanks for your attention

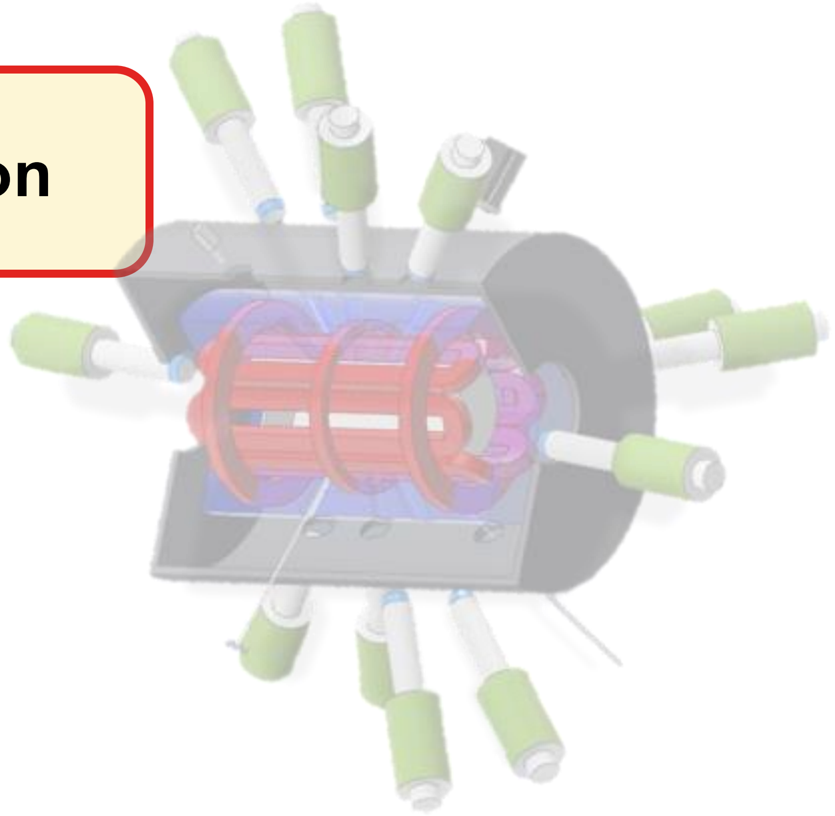

Plasma parameters extrapolation

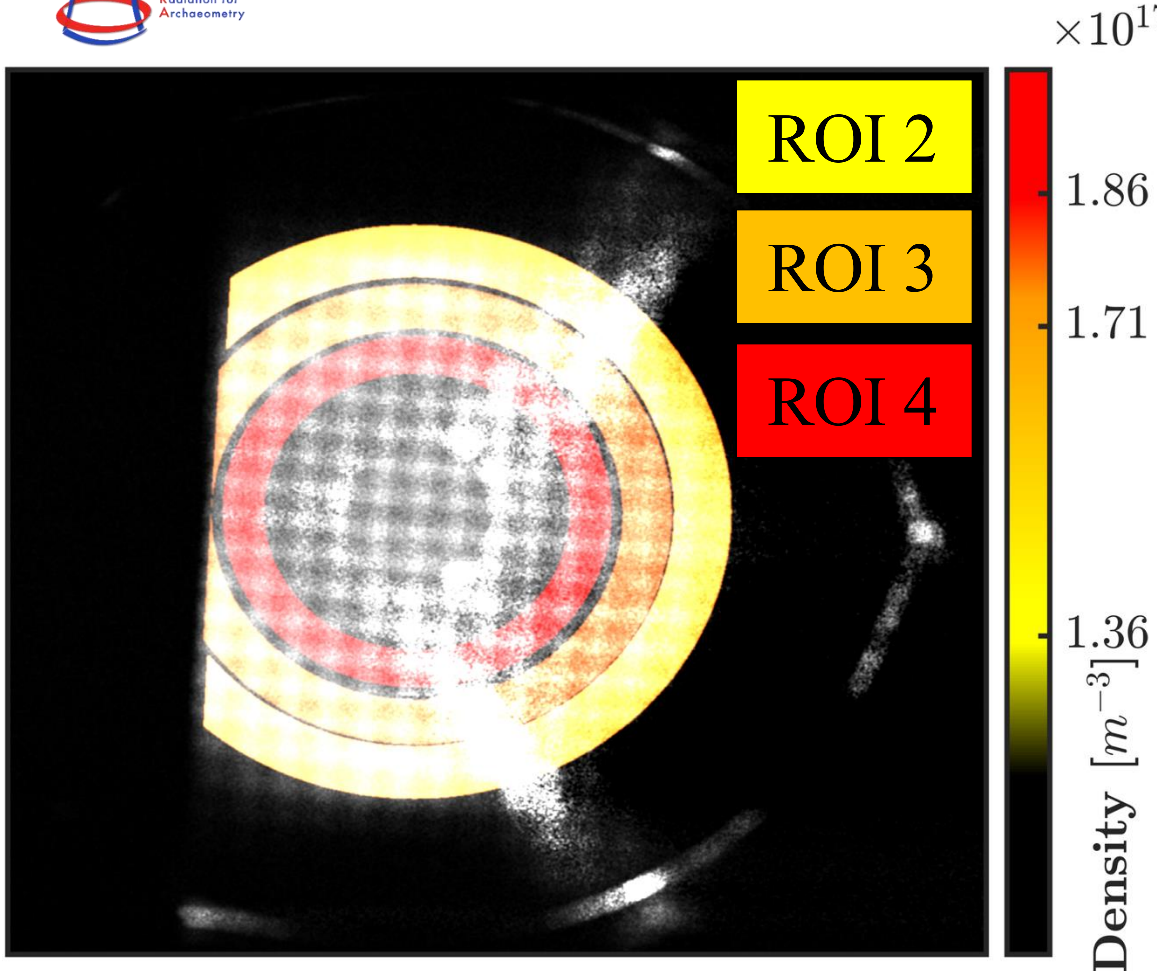

G. Finocchiaro et al., Phys. Plasmas 31, 062506 (2024)

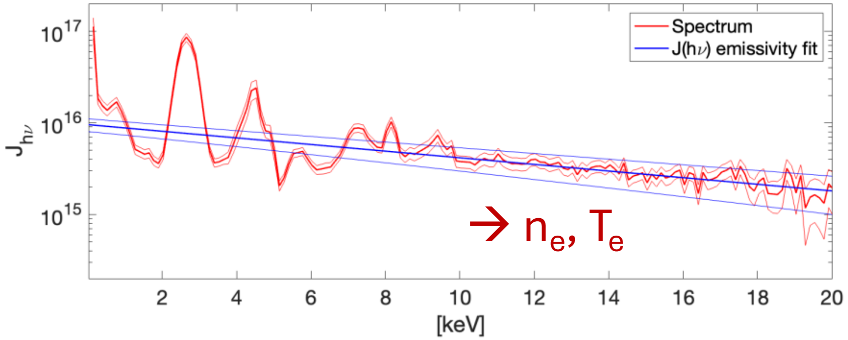

Temperature and **density** values extracted in different image regions

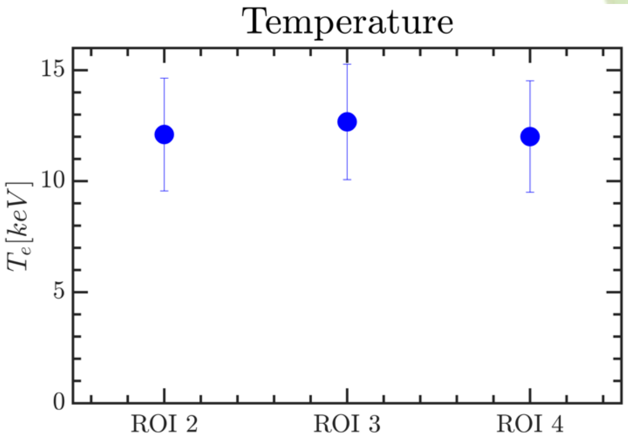

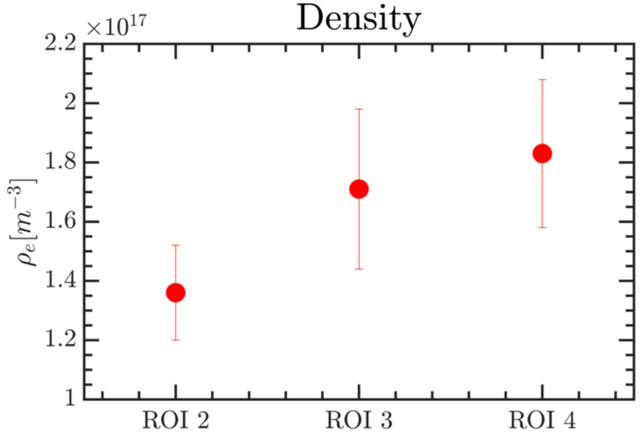

	e- temperature [keV]	e- density [m^{-3}]
ROI 2	12.10 ± 2.54	$(1.36 \pm 0.16) \cdot 10^{17}$
ROI 3	12.67 ± 2.60	$(1.71 \pm 0.27) \cdot 10^{17}$
ROI 4	12.01 ± 2.51	$(1.83 \pm 0.25) \cdot 10^{17}$

Power of this method:

- **Not invasive**
- **Space-resolved**